

**Strategic Environmental Research & Development Program**

Contract: DACA72-99-C-0011

FY 99 Annual Report

March 2000

---

**NONDESTRUCTIVE TESTING OF  
CORROSION UNDER COATINGS**

---

**Program Manager  
Joanne McLaughlin  
Northrop Grumman**

**Spectral Nondestructive Evaluation  
Principal Investigator  
Don Di Marzio  
Northrop Grumman**

**Electrochemical Measurements  
Principal Investigator  
Hugh Issacs  
Brookhaven National Laboratory**

***NORTHROP GRUMMAN***

**Military Aircraft Systems Division  
One Hornet Way  
El Segundo, California 90245-2804**

**DHC QUALITY INSPECTED 4**

**20000720 122**

REPORT DOCUMENTATION PAGE			Form Approved OMB No. 074-0188	
Public reporting burden for this collection of information is estimated to average 1 hour per response, including the time for reviewing instructions, searching existing data sources, gathering and maintaining the data needed, and completing and reviewing this collection of information. Send comments regarding this burden estimate or any other aspect of this collection of information, including suggestions for reducing this burden to Washington Headquarters Services, Directorate for Information Operations and Reports, 1215 Jefferson Davis Highway, Suite 1204, Arlington, VA 22202-4302, and to the Office of Management and Budget, Paperwork Reduction Project (0704-0188), Washington, DC 20503				
1. AGENCY USE ONLY (Leave blank)		2. REPORT DATE March 2000		3. REPORT TYPE AND DATES COVERED Annual Report
4. TITLE AND SUBTITLE Nondestructive Testing of Corrosion Under Coatings			5. FUNDING NUMBERS N/A	
6. AUTHOR(S) Joanne McLaughlin, Don Di Marzio, Steve Chu, Hugh S. Isaacs, Gordana D. Adzic, Doug Hansen				
7. PERFORMING ORGANIZATION NAME(S) AND ADDRESS(ES)  Northrop Grumman Corporation                      Perkin Elmer Corporation  Brookhaven National Laboratory			8. PERFORMING ORGANIZATION REPORT NUMBER N/A	
9. SPONSORING / MONITORING AGENCY NAME(S) AND ADDRESS(ES) SERDP 901 North Stuart St. Suite 303 Arlington, VA 22203			10. SPONSORING / MONITORING AGENCY REPORT NUMBER N/A	
11. SUPPLEMENTARY NOTES No copyright is asserted in the United States under Title 17, U.S. code. The U.S. Government has a royalty-free license to exercise all rights under the copyright claimed herein for Government purposes. All other rights are reserved by the copyright owner.				
12a. DISTRIBUTION / AVAILABILITY STATEMENT Approved for public release: distribution is unlimited.				12b. DISTRIBUTION CODE A
13. ABSTRACT (Maximum 200 Words) Surface corrosion on aluminum aircraft skins, nears joints and around fasteners is often an indicator of buried structural corrosion and cracking. Aircraft paints are routinely removed to reveal the presence of corrosion on the surface of metal structures, and the aircraft is subsequently repainted. This process is expensive, time consuming, and results in the generation of air pollution and process waste. A method is needed to detect the early onset of corrosion on metal substrates covered by protective coatings so that aircraft paints do not have to be stripped without cause. By employing nondestructive techniques to inspect the aircraft exterior structure without removing coatings, the amount of stripping and reapplication of coatings that occurs at the military rework facilities can be substantially reduced.				
14. SUBJECT TERMS SERDP, SERDP Collection, corrosion, coating, spectral nondestructive evaluation (SNDE), wide area spectral imaging (WASI), Scanning Kelvin Probe (SKP)				15. NUMBER OF PAGES 51
				16. PRICE CODE N/A
17. SECURITY CLASSIFICATION OF REPORT unclass	18. SECURITY CLASSIFICATION OF THIS PAGE unclass	19. SECURITY CLASSIFICATION OF ABSTRACT unclass	20. LIMITATION OF ABSTRACT UL	

# **Nondestructive Testing of Corrosion Under Coatings**

**Strategic Environmental Research & Development Program**

**Project Number: 1137**

**FY 99 Annual Report**

**By**

**Joanne McLaughlin, Don Di Marzio, Steve Chu**

**Northrop Grumman Corporation**

**Hugh S. Isaacs, Gordana D. Adzic**

**Brookhaven National Laboratory**

**Doug Hansen**

**Perkin Elmer Corporation**

**March 2000**

*This page intentionally blank*

EXECUTIVE SUMMARY.....	2
INTRODUCTION AND OVERVIEW .....	3
TECHNICAL BACKGROUND .....	5
SPECTRAL NONDESTRUCTIVE EVALUATION .....	5
ELECTROCHEMICAL IMPEDANCE SPECTROSCOPY .....	6
SCANNING VOLTA POTENTIAL MEASUREMENTS .....	6
EXPERIMENTATION .....	8
SAMPLE PREPARATION.....	8
SNDE .....	9
EIS .....	9
SCANNING VOLTA POTENTIALS MEASUREMENT .....	11
RESULTS AND DISCUSSION .....	13
SNDE .....	13
<i>Baseline Measurements.....</i>	<i>13</i>
<i>Corrosion Modeling .....</i>	<i>16</i>
<i>DHR of Corroded Coupons.....</i>	<i>18</i>
<i>Free Standing Paint Films .....</i>	<i>21</i>
<i>SNDE Sensitivity Study.....</i>	<i>23</i>
ELECTROCHEMICAL IMPEDANCE SPECTROMETRY.....	28
SCANNING VOLTA POTENTIAL MEASUREMENTS .....	43
CONCLUSIONS AND FUTURE WORK .....	46
SNDE .....	46
IMPEDANCE MEASUREMENTS .....	46
SCANNING VOLTA POTENTIALS MEASUREMENTS .....	47
ACKNOWLEDGMENTS .....	48
REFERENCES .....	48

## EXECUTIVE SUMMARY

Surface corrosion on aluminum aircraft skins, nears joints and around fasteners is often an indicator of buried structural corrosion and cracking. Aircraft paints are routinely removed to reveal the presence of corrosion on the surface of metal structures, and the aircraft is subsequently repainted. This process is expensive, time consuming, and results in the generation of air pollution and process waste. A method is needed to detect the early onset of corrosion on metal substrates covered by protective coatings so that aircraft paints do not have to be stripped without cause. By employing nondestructive techniques to inspect the aircraft exterior structure without removing coatings, the amount of stripping and reapplication of coatings that occurs at the military rework facilities can be substantially reduced.

This report describes progress made in 1999 for *Task 1- Corrosion Detection and Standards Development*. Three techniques were investigated: spectral nondestructive evaluation (SNDE), electrochemical impedance spectroscopy (EIS) and a scanning probe in a conducting gas (SPG).

The results of the 1999 spectral imaging work indicate that this technique can be used to detect small quantities of corrosion under most conventional coating systems. It has been shown that adequate transmittance is obtained with standard epoxy primers as well as Koroflex (MIL-P-85582, MIL-P-23377, and TT-P-2760). These coatings are typically applied to a thickness range of 0.6 to 0.9 mils. In addition, this technique can "see through" up to 10 mils of a standard, polyurethane topcoat (MIL-C-85285). Only one area of difficulty was encountered during this phase of the program. The data indicates that the aluminum oxide peak does not image well through the sprayable polysulfide primer (MIL-S-81733).

Electrochemical measurements have been made of a range of samples with different surface preparation, coatings before and after exposure to corrosion environments. Two techniques were investigated EIS and SGP to measure Volta or work function difference. A probe was developed to make the EIS measurements on localized areas of coated and uncoated samples. The measurements have shown that scratches in chromate conversion coatings and sulfuric acid anodized aluminum alloys can be detected. SGP measurements have demonstrated that the results obtained with uncoated metals are in good agreement with conventional work function measurements using a Kelvin probe. The SGP method was found to be very sensitive of defects in organic coatings.

## **INTRODUCTION AND OVERVIEW**

Aircraft rework typically involves the stripping and reapplication of coatings applied to protect the outer mold line (OML) of aircraft structure. Recent advances in coating technology are leading to the development of coatings that will last beyond standard depot level maintenance (SDLM) cycles for military aircraft. It is currently feasible to apply corrosion inhibiting primers that provide excellent adhesion properties and are not intended to be routinely stripped. In addition, it is anticipated that the next generation of cleanable, durable topcoats may remain on the air vehicle for extended periods (10+ years). In the past, stripping of the coatings provided a means to visually inspect the condition of the substrate. As we move toward application of more permanent coatings, it is imperative that alternate inspection techniques be developed which can verify the integrity of the coating system and substrate without relying on coating removal.

Over the years, a variety of nondestructive detection methods have been evaluated for detecting corrosion with varying degrees of success. One of the limitations of these previous techniques is their inability to detect relatively small concentrations of corrosion products at the metal/paint interface. Ultrasonic, thermography, and eddy current techniques are useful for crack detection, however, these methods tend to concentrate on detecting significant amounts of bulk corrosion and defects in structural members [1]. This SERDP program addresses the use of technologies and techniques that can be used for detecting changes in the coating system and very small amounts of corrosion under the coatings.

The objective of this SERDP program is to develop nondestructive inspection techniques to locate hidden corrosion on aircraft surfaces without requiring removal of the coating. Several techniques have been identified that can achieve this: imaging of the surface using spectral nondestructive evaluation (SNDE) and wide area spectral imaging (WASI), and scanning reference electrode measurement techniques using instrumentation such as the Scanning Kelvin Probe (SKP).

For the SNDE portion of the program, the bulk of the effort in 1999 concentrated on:

- a) establishing baseline spectral properties relevant to corroded aluminum aerostructures;
- b) gauging quantitative spectral measurement through modeling of corrosion and salt fog exposure for variety of surface treated aluminum coupons;
- c) spectral evaluation of coated panels;
- d) analysis of the corrosion signature sensitivity.

For the two electrochemical measurement techniques efforts in 1999 concentrated on:

- a) development of the impedance measurements probes;
- b) development of measurement techniques optimized for field detection of corrosion underneath a paint;
- c) performing Volta potential measurement using conventional Kelvin probe methods and with conducting gases and baseline against measurements obtained using the Kelvin Probe.

The following sections describe these novel inspection techniques for detecting corrosion under a paint film and the progress made toward meeting the objectives of this program.



## TECHNICAL BACKGROUND

Corrosion can occur at a variety of locations on an aircraft. These include joints, fasteners, and repairs, as well as skin surfaces exposed to harsh environments (i.e., sea spray). A variety of aircraft at Northrop Grumman's facility in St. Augustine, Florida were examined, included the E2C and the EA6B, which are primarily carrier based aircraft and are consequently exposed to sea spray and salt fog. Corrosion was found to concentrate around joints, fasteners, and in areas where water could accumulate. Extensive corrosion causes obvious blistering to the paint, but incipient corrosion could not be detected visually.

The following paragraphs provide background information and descriptions for each of the nondestructive corrosion detection and measurement techniques evaluated to date by this program. Wide Area Spectral Imaging (WASI) is not included since work in this area will start in the following year.

### SPECTRAL NONDESTRUCTIVE EVALUATION

SDNE uses directional hemispherical reflectance (DHR) to determine the spectral properties of surfaces. As shown in Figure 1, a collimated IR beam in the range of 1.8 to 15.4  $\mu\text{m}$  is directed near normal to the surface, and then the reflected light, both specular and diffuse, is measured in an integrating sphere. Reflectance is plotted as a function of wavelength or wavenumber. It is important to collect the diffuse component of the reflected light since the reflectance signal from any corrosion at the metal surface will be significantly scattered by the overlying paint layer.

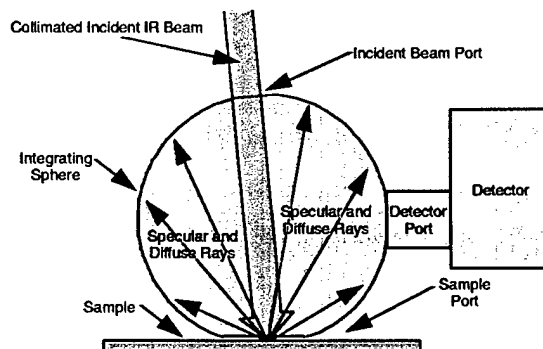


**Figure 1** Integrating sphere system used to measure directional hemispherical reflectance.

The SNDE technique depends on the generation of a database for the spectral signatures of corroded surfaces. Baseline reflectance measurements for clean, uncoated aluminum alloys are compared to measurements made on corroded panels in order to identify and quantify corrosion byproduct signatures. Similarly, the reflectance through typical aircraft coatings must be measured and characterized. Using this database and appropriate analysis techniques should enable identification of corrosion on painted aircraft structure.

### ***ELECTROCHEMICAL IMPEDANCE SPECTROSCOPY***

Electrochemical techniques for the detection and quantification of corrosion under paint films historically have involved AC impedance and DC measurements, requiring the immersion of the samples in an electrolyte [2]. This program is studying an electrochemical measurement technique that requires no electrolyte (in liquid form), and therefore no direct contact with the sample.

The objective of this research is to determine the ability of EIS to make localized measurements that detect corrosion under coatings and to develop simplified techniques to perform field measurements. The apparatus used for the measurements being reported consisted of components designed to form an electrochemical cell using a conducting gas, which will potentially be used for corrosion measurements at aircraft surfaces.

### ***SCANNING VOLTA POTENTIAL MEASUREMENTS***

Recently the scanning Kelvin probe has been employed, highly successfully, as a non-contacting technique for the measurement of Volta potentials in studies of corrosion under coatings [3,4,5]. The scanning Kelvin probe consists of a vibrating microelectrode close to a surface to produce a variable capacitance that induces an AC signal in the circuit directly connecting the probe and surface. Intrinsically, the method has a high impedance and necessitates both scanning close to the surface being studied, and care in shielding to reduce electrical noise. In contrast to the well-known Kelvin probe method, direct (DC) measurements of the Volta or contact potential difference have been made in ionized air by Case and Parsons [6] and Smith [7]. In these studies, a radioactive  $\alpha$  emitting source was used to ionize the air between the

reference metal/gas electrode and a gas/solution interface [6] or a second gas/metal electrode [7].

X-ray ionization of a gas is initiated by a primary x-ray absorption photoelectric process and is followed by ionization caused by ejected secondary electrons. Electron and fluorescent photon emission takes place in the gas around the site where the beam impinges on the metal and increases the ionization. Ionization by the electrons continues until they have lost their energy and attach to molecules. The process produces negative and positive charged gaseous molecules that combine and interact to form a range of products. Recombination of the ions and secondary electrons takes place rapidly as they diffuse from the path of the x-ray beam. The high concentration of charged species can be detected over distances of the order of a few 0.1 mm and depend on pressure and gas composition [8,9,10].

The present task is using the DC ionized-air technique to the measure the Volta potential to with the view to locate corrosion under coatings. It is similar to a localized DC electrochemical measurement of the corrosion potential and hence may be able to locate corrosion sites. In order to obtain a conducting gas we have used high intensity synchrotron x-rays to produce a local ionized atmosphere adjacent to the metal surface under investigation. The technique has advantages over conventional Kelvin probe as it greatly simplifies the Volta potential measurements. In particular, Volta measurements using ionized air are relatively insensitive to reference/sample distances. Thus, the need for complicated electronics to maintain a constant height above the surface is avoided. Additional advantages are relatively low impedance even with a small reference electrode, and the ability to carry out electrochemical (current versus voltage) polarization measurements of the metal/conducting-gas interface.

## **EXPERIMENTATION**

### ***SAMPLE PREPARATION***

The test specimens used for the validation of the measurement techniques were manufactured in the Northrop Grumman Material & Process Laboratory. The specimens were prepared using aluminum alloys that are most typically found on the aircraft outer mold line (OML); specifically, 2024-T3 Bare (Al2024), 2024-T3 Clad (Al2024C), 7075-T6 Bare (Al7075) and 7075-T6 Clad (Al7075C). Surface Preparations included both chemical conversion coating (CCC), applied per MIL-C-5541 and sulfuric acid anodize (SAA), applied per MIL-A-8625 Type II. The bottom half of the specimens (4" x 6") were scribed down to the base metal to provide an area that would be more susceptible to corrosion upon exposure to the salt spray or humidity. Different exposure durations were used to induce varying degrees of substrate corrosion. The salt spray exposure proceeded for 3, 7, 10 and 14 days. The humidity exposure proceeded for 3 days, 7 days, 10 days, 2 weeks, 4 weeks and 6 weeks. These specimens were used to baseline and quantify the various changes that occur in the substrate due to the varying levels of corrosion. Both untreated and unexposed SAA and CCC specimens were prepared to provide a baseline for untreated aluminum, unexposed CCC, and unexposed SAA.

Coupon samples of the coating schemes currently applied to F-14, E-2C, EA-6B, and F-5 were prepared to represent the "as applied" coatings. These included MIL-P-85582 Type II, TT-P-2760, MIL-S-81733, MIL-C-85285 (16440, 36375, 36320, 35237). To simulate the barrier provided by these coatings, free-standing paint films were prepared using MIL-P-85582, TT-P-2760, MIL-C-85285, and MIL-S-81733 over the range of 1 to 10mils. Using the IR imaging technique, the directional hemispherical reflectance of the free-standing films was determined. The films were then placed over the pre-corroded specimens to the appropriate coating stack-up.

Field hardware for the first phase of the component evaluation was obtained from Northrop Grumman's St. Augustine site. Scrap E-2C access doors were selected for this portion of the study. The access doors have a complex curvature and have rivet holes located around the outer edges. The surface preparation used in the manufacture of the doors is SAA. Fasteners made of a noble metal will be installed in selected holes to induce corrosion upon exposure to salt fog per ASTM B117.

### **SNDE**

In order to determine the sensitivity of SNDE to such factors as the amount of corrosion present, the type of aluminum surface treatment, and the type and amount of paint coating present, we decided to measure these aspects separately. Unpainted aluminum coupons with surface treatments were corroded and their spectral reflectance measured. Corrosion was modeled using an alumina powder contamination technique. Likewise, free standing paint films were fabricated and their transmittance and reflectance were measured as a function of type and thickness. Finally, the films were applied to the corroded substrates to determine how much corrosion can be seen through a variety of coating thicknesses.

### **EIS**

Samples with three surface conditions are being evaluated: defect free coatings, coatings with scribes, and these surfaces after exposure to corrosion conditions. Our goal is to detect and characterize the surfaces by using EIS technique. The EIS investigation in 1999 was conducted on the samples prepared as previously described in this section. EIS experiments were performed with the aim to simplify the measurements, to avoid immersion of the sample in liquid electrolyte and to shorten measuring time. Such technique was able to detect a big difference in impedance between the scribed and intact spots on the samples after different exposures to corrosive environment.

A special probe consisting of a reference and a counter electrode was designed for the impedance measurements. A copper disk was used as a counter electrode with an insulated embedded small silver disc in the middle, serving as a reference electrode (Figure 2). Filter paper placed between sample and a probe served as the electrolyte container. The copper disk acted as the second electrode in two electrode cell measurements. The working area of the surface whose impedance is measured is determined by the size of counter electrode and filter paper ( $3.14 \text{ cm}^2$ ). A series of sponges were tried as alternatives to the filter paper but these were not as reliable as the filter paper and required recesses in the copper disk to hold the sponge.

Experiments were performed with non-aggressive borate solution pH 8.4, 0.1M  $\text{Na}_2\text{SO}_4$  and with a more aggressive electrolyte, 0.1M  $\text{NaCl}$ . The measurements were made using a Solartron Electrochemical Interface Model 1287 in combination with Solartron Frequency Response Analyzer Model 1250.

The amplitude of the modulating signal was 30 mV with the frequency in the region from 0.01 to 50 kHz Spectra are presented in the form of Bode plots and Nyquist plots for data at high frequencies. All results reported were obtained in the potentiostatic mode at the corrosion potential.

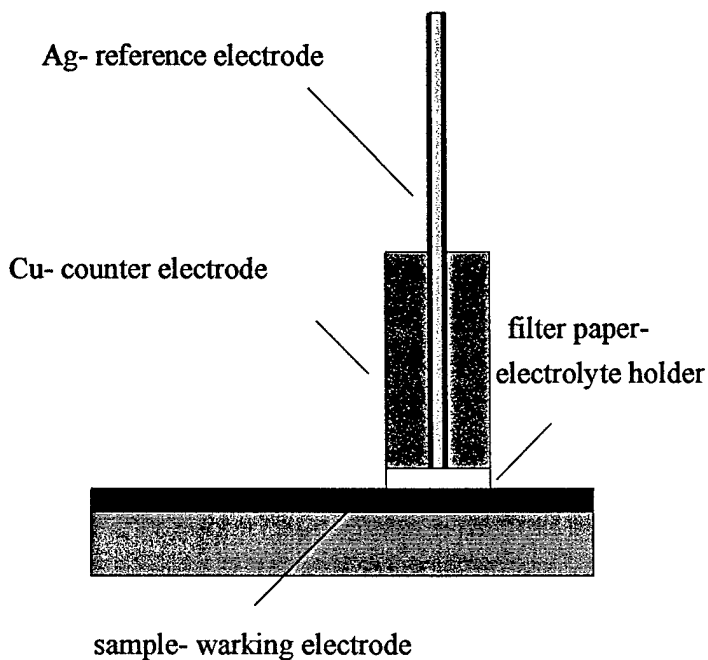


**Figure 2** Schematic of electrochemical cell for localized impedance measurement

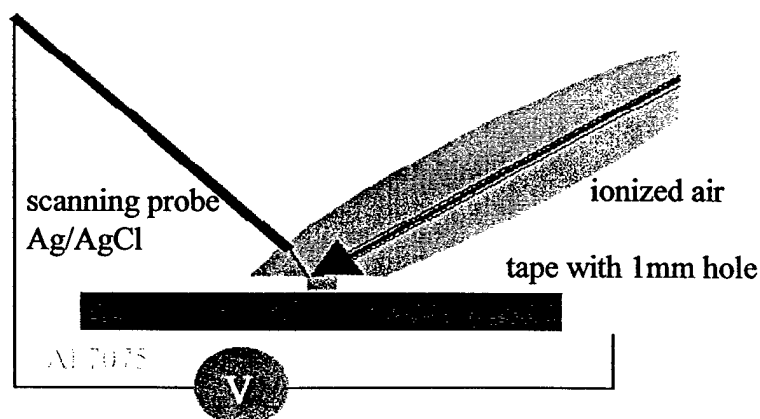
## SCANNING VOLTA POTENTIALS MEASUREMENT

A multi-metal specimen was used to demonstrate the technique using x-rays. It consisted of the abraded edges of a series of metal sheets about 1 to 4 mm thick, pressed together in a holder. The metals were type 304 stainless steel, Al, Ni, Zr, Cu, Sn, and Fe. The specimen was abraded on SiC paper down to a 600 mesh. Care was taken to prevent cross contamination of adjacent metals during the final abrasion of the sheet cross sections.

A schematic of the measuring setup is shown in Figure 3. In this system, the beam is 45° to the sample. A stepper motor driven x-y-z stage with a minimum step size of 1  $\mu\text{m}$  was used for positioning the sample. A reference electrode probe was positioned about 0.1 mm from the sample. Generally, the reference probes were parylene coated, 0.25 mm diameter Pt-20% Ir alloy wires with exposed cross sections positioned 0.1 mm above the sample. Ag and Ni wire reference probes were also used with equal success.

Volta potentials were also measured using an EG&G Scanning Kelvin Probe System 100E with a Ni scanning electrode having a tip diameter of 0.1 mm. The measurements were made at Beamline X26A and X19 at the National Synchrotron Light Source. The X26A is designed for x-ray microprobe measurements using either monochromatic or polychromatic x-rays. The monochromatic beam has a photon flux of about  $10^4$  photons  $\text{s}^{-1}\mu\text{m}^{-2}$  for an x-ray ring current of 200 mA. The beam was focused to a diameter of close to 25  $\mu\text{m}$ . The diameter of the polychromatic beam was about 8  $\mu\text{m}$  with a flux of about  $10^8$  photons  $\text{s}^{-1}\mu\text{m}^{-2}$  having energies above 4 keV at a ring current of 200 mA [11]. The measurements on X19 were at a fixed energy of usually 6090 eV and up to 1x2 mm in size although apertures collimating the beam have been used.

**Figure 3 Schematic of the Volta potential measurements in ionized air**







## RESULTS AND DISCUSSION

### SNDE

The DHRs of a variety of surface treated aluminum coupons were measured in order to generate a spectral database of substrate reflectance. This will tell us how much change in reflectance we can expect from a certain amount of corrosion present. Once this has been established, a first cut at corrosion sensitivity will be determined using free standing paint films covering corroded coupons.

### BASELINE MEASUREMENTS

Figure 4 and Figure 5 show the DHR of a number of as-prepared (uncorroded) representative 3" X 6" aluminum coupons. Two aluminum alloys, 2024 and 7075, were used in both bare and clad form. The 2024 alloy exhibits more corrosion resistance than does 7075 alloy. Clad coupons in general have better resistance than unclad coupons. In addition, two types of surface coatings were used, sulfuric acid anodized (SAA) and Alodine 1200 chromated conversion coating (CCC). The SAA coupons are expected to show more corrosion resistance than those prepared with CCC.

Figure 4 shows higher reflectance for the CCC clad coupon compared to the unclad. This indicates that there is some transparency in the CCC. This is also true for the SAA coated coupons shown in Figure 5. In both cases, the reflectance difference is relatively small. The corrosion products will have to make their way through the coating to the primer for the SNDE technique to be able to "see" any significant corrosion.

Figure 6 shows a comparison of the two as prepared surfaces (SAA and CCC, with the DHR of a bare salt fog corroded 2024 aluminum coupon. The corrosion products, shown in the scanning electron microscope (SEM) image in Figure 7, appear as a white patina on the surface. Analyzed by electron microprobe (EDAX), the corrosion products are essentially aluminum oxide ( $\text{Al}_2\text{O}_3$ ) with excess oxygen and some trace amounts of sodium, magnesium, and chlorine from the salt spray. There is a similarity in all three reflectance spectrums. This is especially so in the 3400  $\text{cm}^{-1}$  region. This is the absorption band from hydroxyl groups, which are found bound to oxides. As the oxide layer increases due to weathering, this hydroxyl absorption increases. It is no surprise that hydroxyl absorption is also found in the SAA and CCC, as these also tend to bind hydroxyl groups.

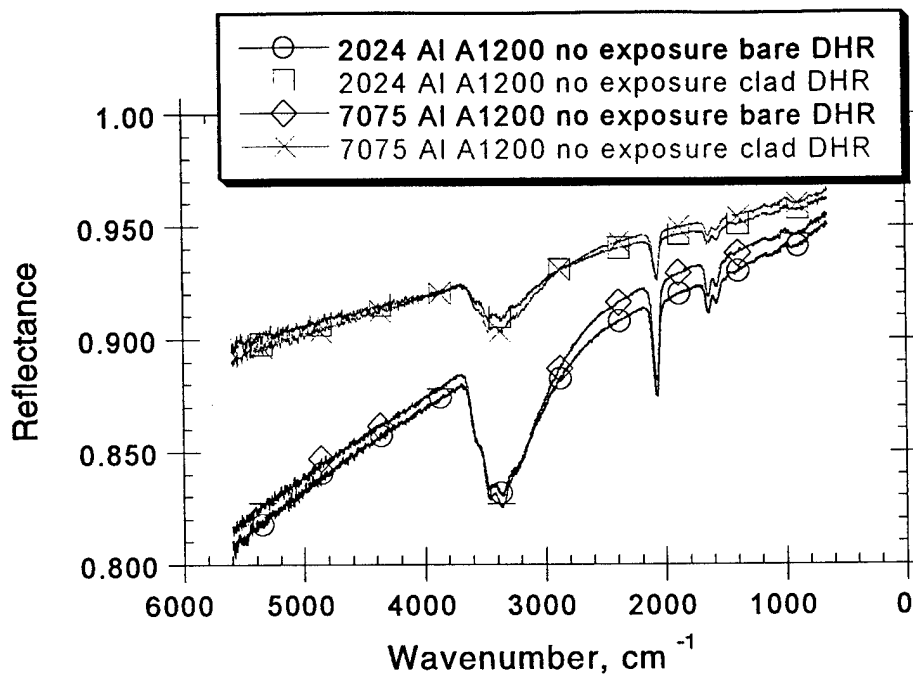


Figure 4 DHR of 2024 and 7075 bare and clad aluminum 3" X 6" coupon, coated with CCC.

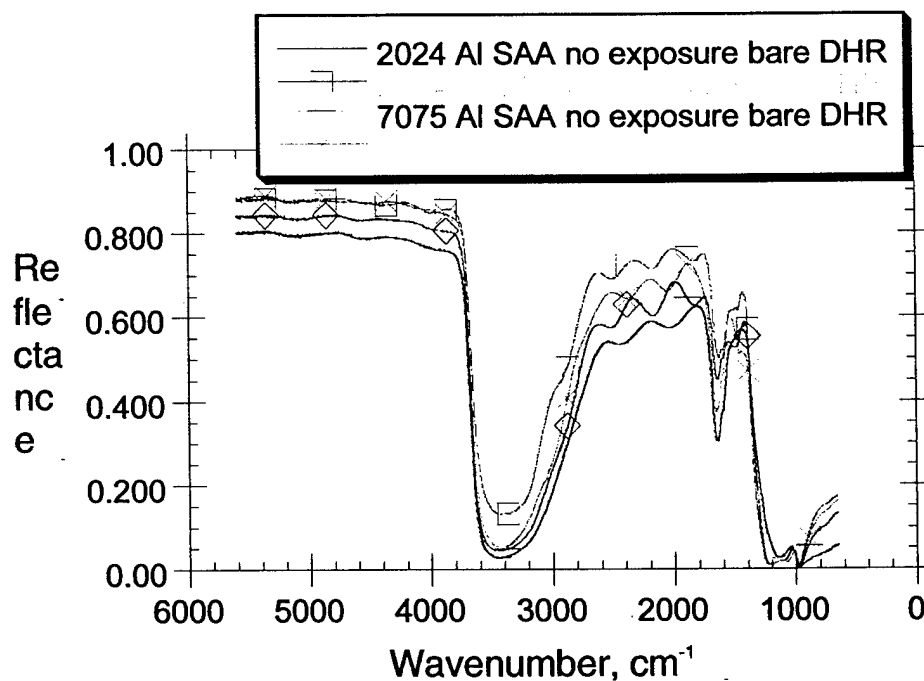


Figure 5 DHR of as prepared sulfuric acid anodized 2024 and 7075 bare and clad aluminum coupons.

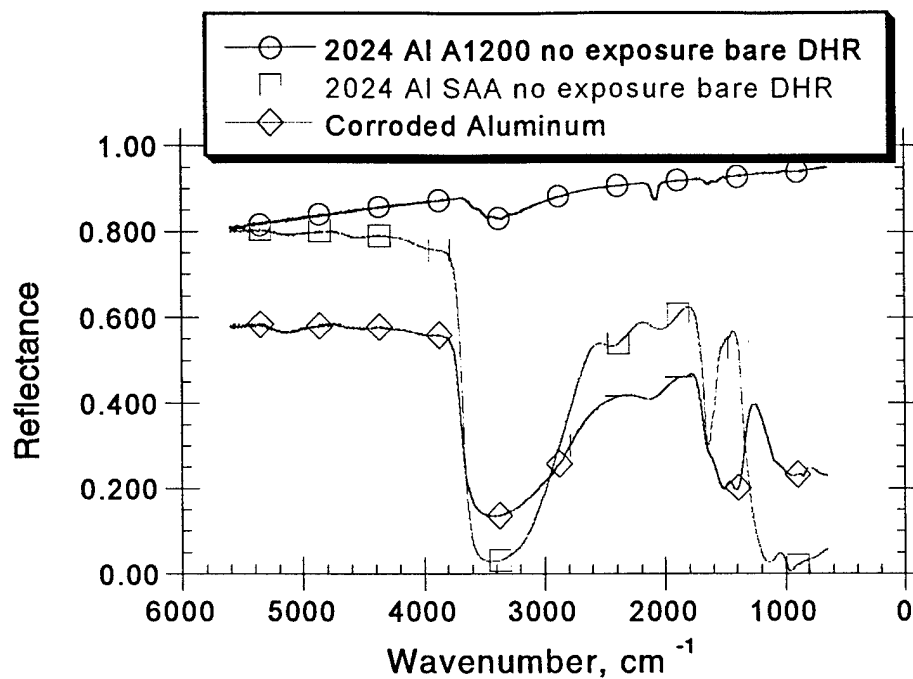


Figure 6 Comparison of as prepared coated 2024 bare aluminum with salt fog corroded 2024 aluminum.

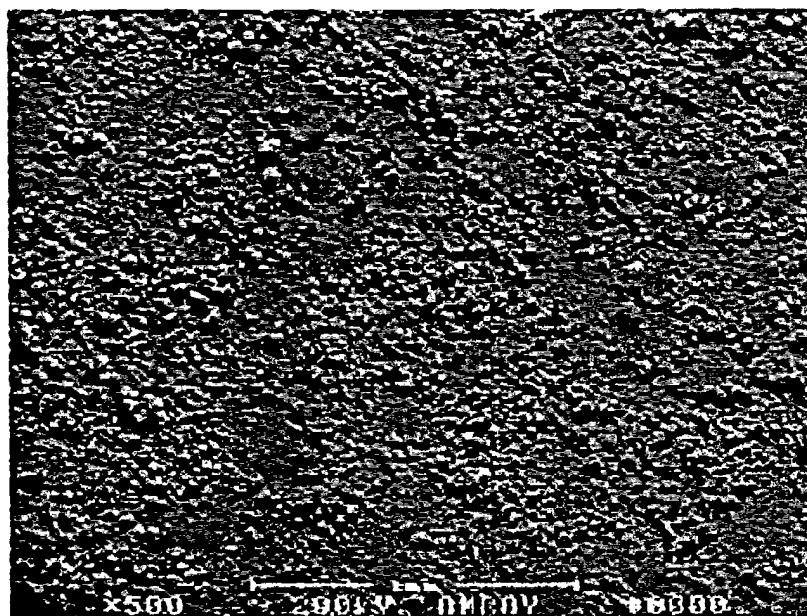


Figure 7 Scanning electron micrograph of a salt fog corroded bare aluminum coupon. Oxide is primarily  $\text{Al}_2\text{O}_3$ .

Accelerated weathering was performed in both humidity and salt fog chambers. "X's" were scribed into the surface of each coupon to promote

corrosion. Samples were initially weathered for 3 to 14 days. In addition, large regions of coated aluminum coupons were extensively weathered to approximate an aluminum sheet with a significant amount of corrosion damage.

### CORROSION MODELING

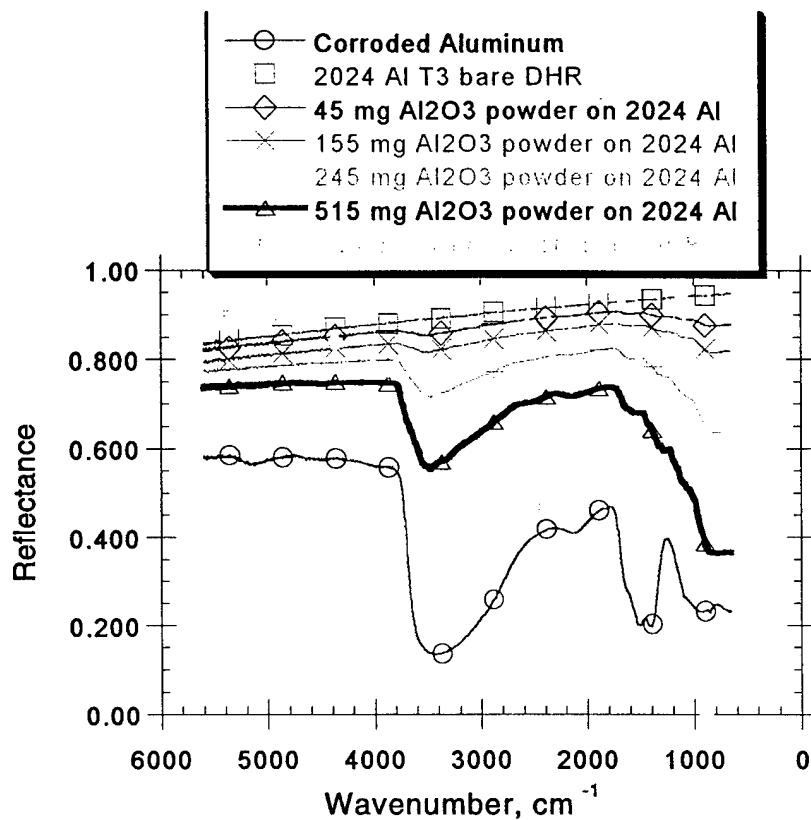
An alumina contamination study on aluminum alloy sheets was performed to quantify the amount of corrosion present using spectral reflectance techniques. Accelerated corrosion, induced by exposure to salt spray, is essentially a layer of  $\text{Al}_2\text{O}_3$  (alumina) on the surface. This can be approximated by sprinkling successive amounts of  $\text{Al}_2\text{O}_3$  powder on an aluminum surface and measuring the DHR. The series of spectra are used to model the DHR of a corroded aluminum sample. By measuring the reflectance, an approximation can be made as to the amount of corrosion present. Depending on the sensitivity and signal-to-noise found in the SNDE technique, this can be used to obtain a quantitative determination of the amount of corrosion present.

Figure 8 shows a series of DHR spectra of a bare aluminum (uncoated) coupon covered with  $\text{Al}_2\text{O}_3$  powder. The powder was from Aldrich with a nominal grain size of 1 micrometer. As the amount of  $\text{Al}_2\text{O}_3$  coverage increases, the DHR approaches that of an "infinitely" thick  $\text{Al}_2\text{O}_3$  layer in the spectral region below  $4000\text{ cm}^{-1}$ . Above  $4000\text{ cm}^{-1}$ , the reflectance of the thick powder layer is higher than the thinner layers which indicated some degree of multiple reflection is at work. A theory of optical reflectance and transmission of particulate and diffusive surfaces known as Kubelka-Munk (KB) is frequently used to model such systems. KB theory will be discussed further in connection to modeling the optical properties of paint layers later, but for the  $\text{Al}_2\text{O}_3$  contamination study a simpler area fraction model will be used.

The reflectance,  $R_t$ , of a particulate ( $\text{Al}_2\text{O}_3$ ) contaminated surface (aluminum) is given by Equation A:

$$\text{Equation A} \quad R_t = R_p + (R_s - R_p)e^{(-ad)}$$

where  $R_p$  is the reflectance of an optically thick ("infinite") layer of  $\text{Al}_2\text{O}_3$  powder,  $R_s$  is the reflectance of the substrate (aluminum),  $a$  is a scattering factor, and  $d$  is the average oxide thickness. This area fraction model works well for a large variety of particulate contaminants and substrates.



**Figure 8** Reflectance of  $\text{Al}_2\text{O}_3$  oxide on 3" X 6" aluminum coupon. Corroded aluminum coupon included for comparison.

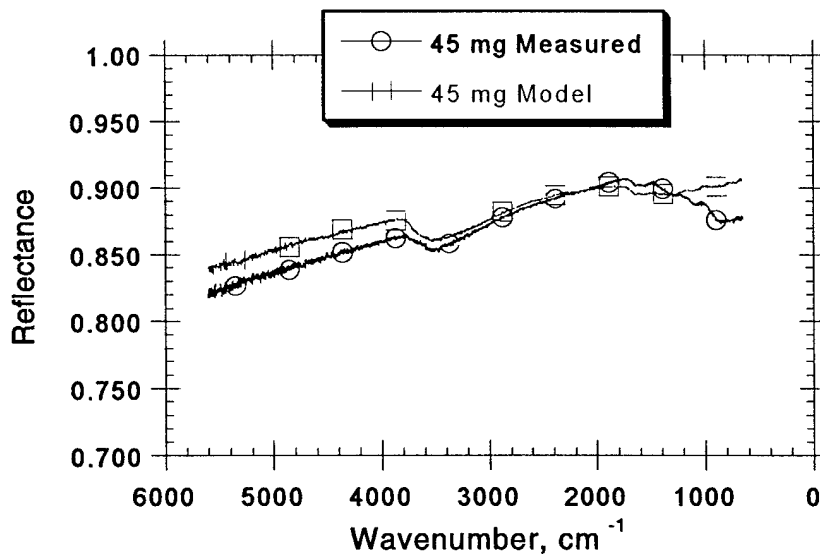


**Figure 9** Measured and Modeled "Corroded" aluminum substrate. 45 mg  $\text{Al}_2\text{O}_3$  powder on 3" X 6" aluminum coupon.

Figure 9 shows a comparison of the area fraction model with the measured reflectance of the  $\text{Al}_2\text{O}_3$  contaminated surface. The model uses the end point spectra (bare aluminum and thick  $\text{Al}_2\text{O}_3$  DHR) as well as a scattering factor derived from the measured spectral shown in Figure 6. There is reasonable agreement between the modeled and measured spectra. For larger amounts of  $\text{Al}_2\text{O}_3$  (thicker oxide), there is some deviation above  $4000\text{ cm}^{-1}$  due to multiple reflectance effects. Of course, real world corrosion differs somewhat from this idealized model, but we can still get an idea of the magnitude of corrosion present.

### DHR OF CORRODED COUPONS

The DHR system used to implement the SNDE technique has an incident IR beam diameter of approximately 0.5"; hence, a five-spot-average reflectance was measured from the scribed coupons. The DHR was measured over the center of the scribe "X", as well as over the four legs of the "X", in order to maximize the amount of corrosion that may be detected. Initial measurements indicated that the corrosion measured correlated with the type of aluminum, coating, and weathering. The most susceptible combination to corrosion was salt fog weathered Al7075, and the least susceptible was humidity exposed, Al2024C. However, in all cases for the maximum exposures made, the amount of corrosion generated was not large and the change in reflectance was not great. Figure 10 show the reflectance's of a series of salt fog exposed, CCC Al7075 coupons. There is a general trend to a growing hydroxyl absorption band, as is expected from a growing oxide layer. It should be pointed out again these measurements consist mostly of reflectance from nominally uncorroded regions with no scribe and a relatively narrow region of corrosion where the scribe is present. Figure 11 shows representative DHR measurements of salt fog exposed SAA coated bare coupons. There is some reduction in reflectance reflecting a growing amount of oxide but not much. These coupons were subsequently returned to the environmental chambers for further weathering.

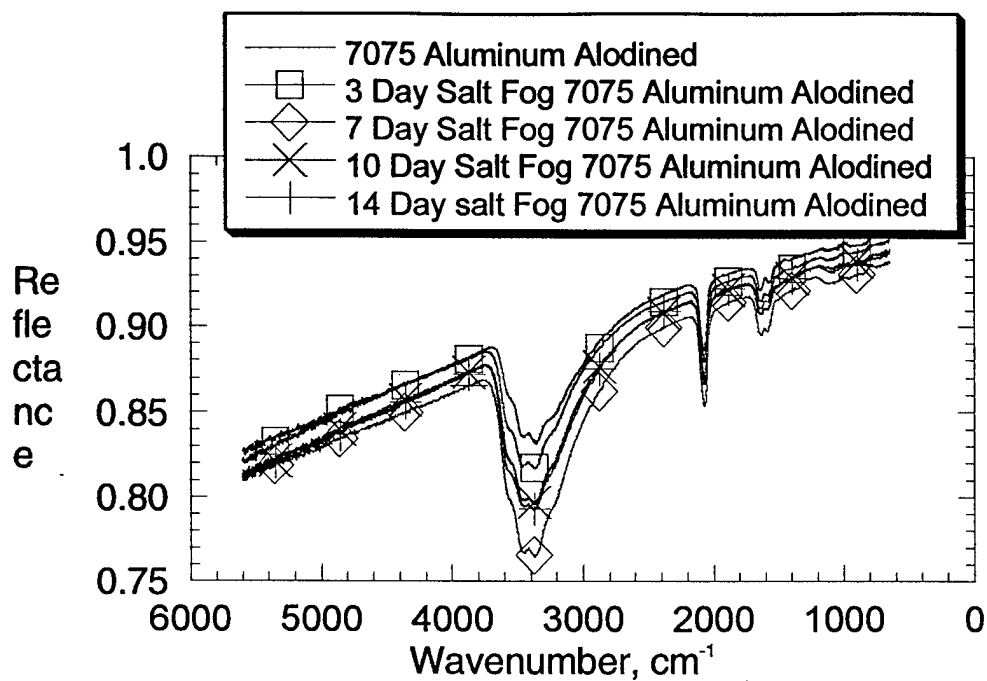


Figure 10 DHR of salt fog exposed, CCC Al2024

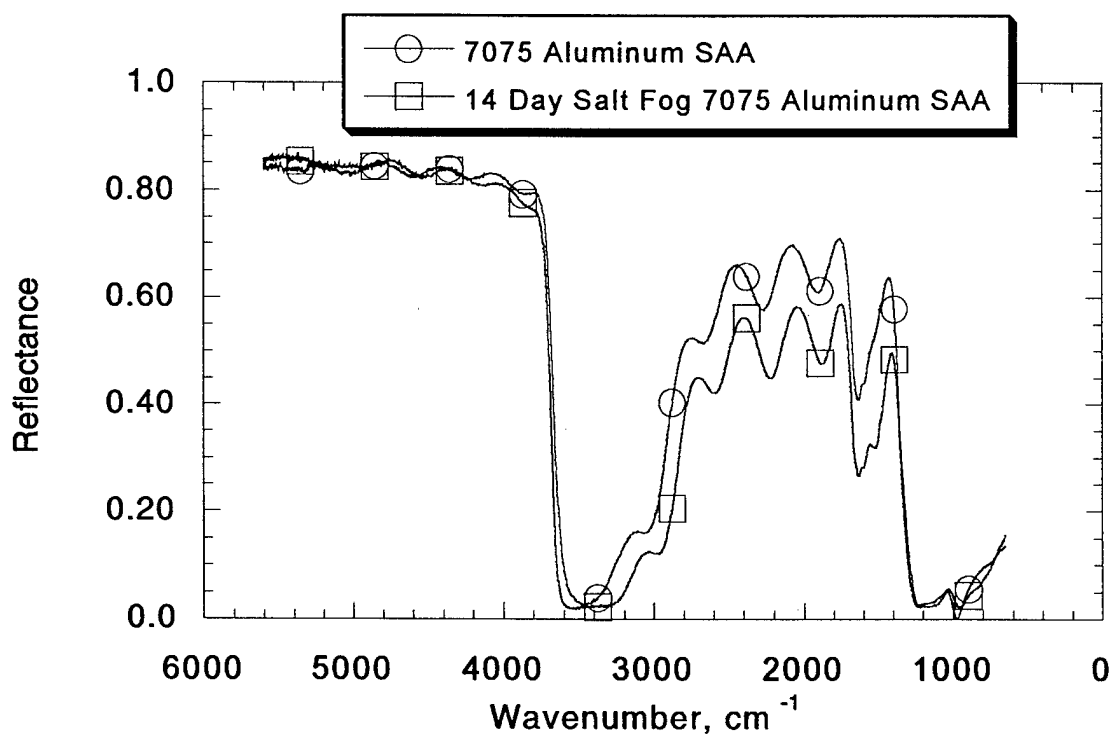


Figure 11 DHR of salt fog exposed SAA coated Al7075.

Because the most extensive corrosion was caused by salt fog exposure, we made a series of coated coupons to expose a 2" X 2" square center. These coupons were given a strong salt fog treatment. Figure 12 shows the reflectance of these coupons. Like the salt fog exposed 2024 uncoated coupon described before, these samples show a strong corrosion signature. Electron microprobe results show the presence primarily of  $\text{Al}_2\text{O}_3$  with some trace amounts salt.

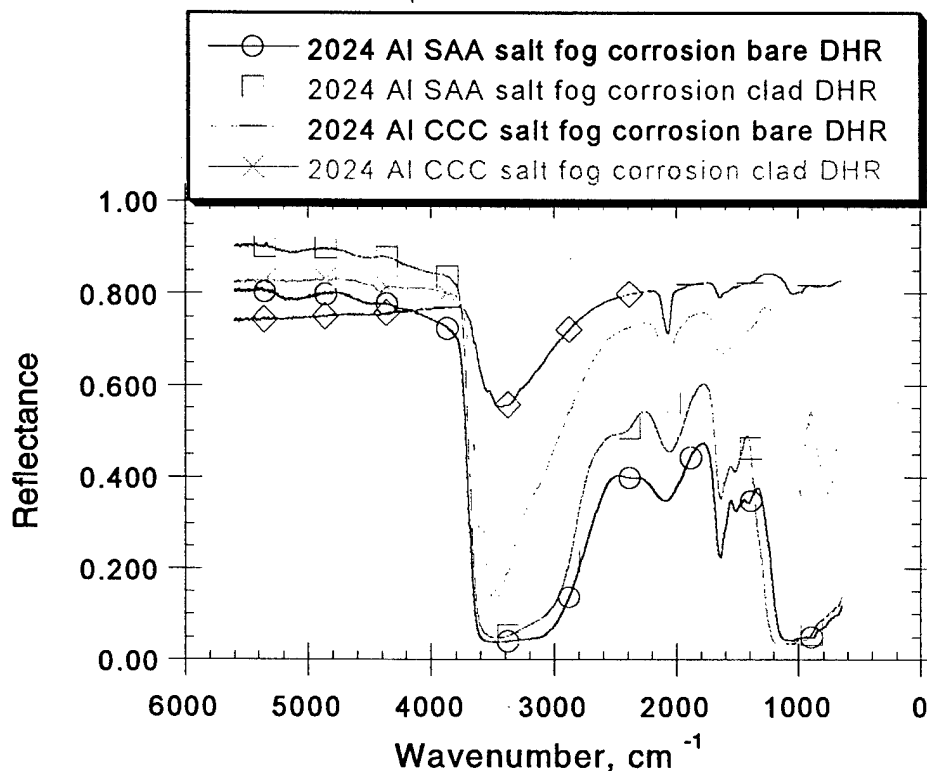


Figure 12 Long-term salt fog exposed heavily corroded CCC and SAA coupons.



### FREE STANDING PAINT FILMS

In order to relate the reflectance of painted corroded aluminum to the corrosion at the metal/paint interface, free standing paint films of a variety of types and thickness' were applied to a characterized corroded surface. In order to get quantitative results that can be modeled; the reflectance and transmittance of these films by themselves were first measured. These quantities, along with the reflectance of the corroded aluminum substrate (coupon), are used to predict the reflectance of the painted coupon.

Figure 13 shows the directional hemispherical reflectance (DHT) of a series of freestanding topcoats and sealants used on aircraft such as the Northrop Grumman EA6B and E2C. DHT measures the amount of the transmitted light including the diffuse scattered component. The thickness shown reflects actual application thickness' on painted airframes. The camouflage gray and gloss gray topcoats exhibit a high degree of transmissivity in the  $2200\text{ cm}^{-1}$  region. This is the "window" where we hope to see through to the aluminum substrate. The Koroflex sealer, which is used on some aircraft, also has a transmissive window in the same region, but at a significantly lower value. The polysulfide sealer transmits about 5% in this region and is essentially opaque for our applications.

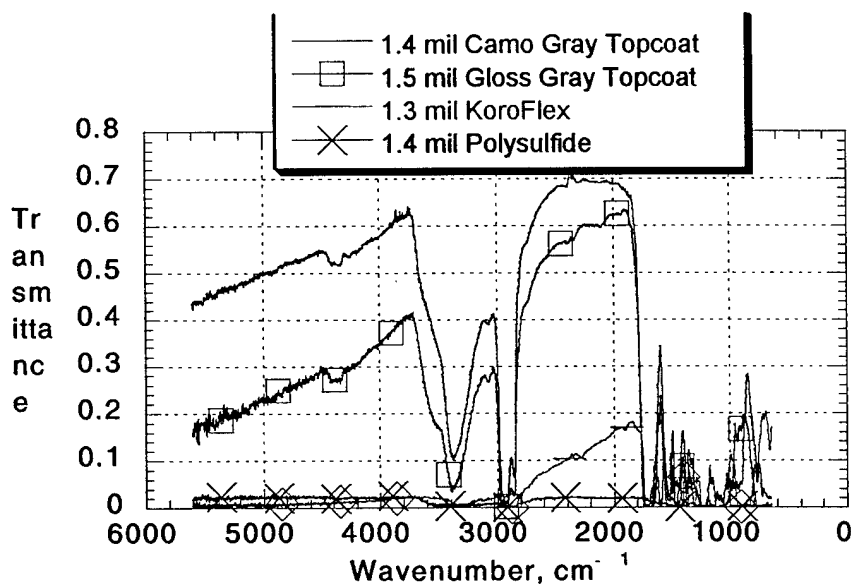


Figure 13 Directional hemispherical transmittance of topcoats and sealers.

Figure 14 shows the DHT of a series of thickness for the camouflage gray topcoat. This topcoat is transmissive up to a thickness of approximately 10 mil. These results also hold for the gloss gray topcoat. In addition to the DHTs, the DHRs of the freestanding coatings was measured with no backing (no substrate). This also included the reflectance of an "infinitely" thick layer (where the DHT is effectively zero). These measurements were necessary as inputs for the model to be described below.

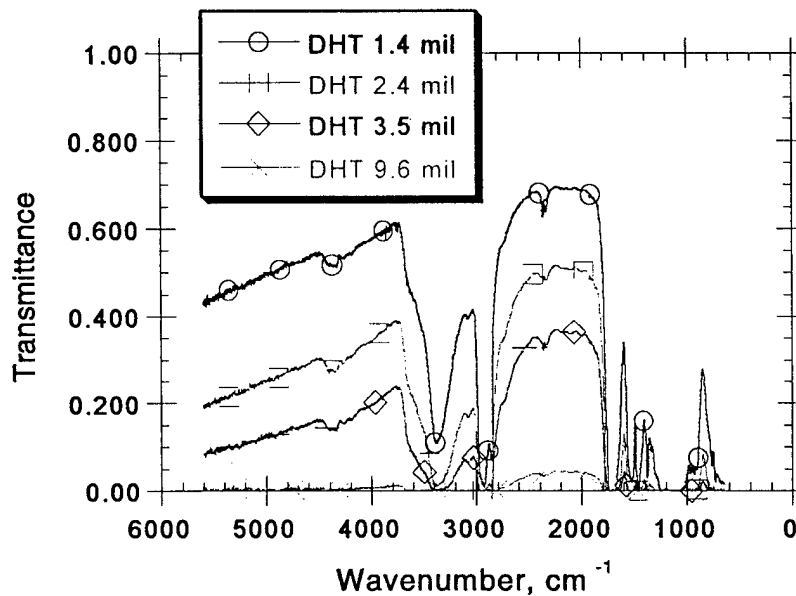


Figure 14 Transmittance of a series of camouflage gray free standing paint films.

### SNDE SENSITIVITY STUDY

For the initial sensitivity study, the long-term salt fog exposed aluminum plate describe above was used as the substrate. This represented an amount of corrosion that could eventually lead to structural damage, but not so much that it would cause visibly obvious blistering to the paint layer covering it. Initial work was done with the free standing camouflage topcoat. Figure 15 and Figure 16 show the DHR for a series of camouflage topcoat films of various thicknesses atop uncorroded and corroded aluminum substrates, respectively. The prominent reflectance peak around  $2200\text{ cm}^{-1}$  is the result of the substrate reflecting the IR light through the transmissive window of the paint. This is clearly seen from both the uncorroded and corroded substrates. Clearly, the signature of corrosion in the substrate is folding into the overall reflectance of paint on substrate combination.

Reflectance's of painted surfaces have been traditionally modeled using a diffusive two beam propagation model. The solution to this model was first found by Kubelka and Munk (KB). The KB model describes the transmission and reflectance of a completely diffusive (lambertian) scattering layer. This layer may also have an opaque but diffusely scattering substrate underneath. This approach has been taken in the past to analyze paintings. Here, the art conservator is interested to see the original charcoal drawing on the canvas surface. Known as infrared reflectography, near IR (up to 2 micrometer) images of a painting are taken. The paint layers, which are opaque in the visible, become partially transparent in the IR, and the underlying drawing is revealed.

One of the problems inherent in the KB model is the assumption of a totally diffusive surface. This implies that there is not an abrupt smooth boundary between the air and the paint surface with a corresponding change in index of refraction. This is clearly not the case for aircraft paints. Paint consists of an organic binder and a light scattering pigment, and the binder by itself has an index of refraction in the area of  $n = 1.5$ . The sudden change from air ( $n = 1.0$ ) to the binder will cause a portion of incident light to be reflected at this boundary, independent of the diffusely scattering pigment. This effect is not included in the KB model. Multiple reflection from this boundary and a specular (non-diffuse) reflection from the paint/substrate interface are also not included. Attempts to use the KB model to simulate transmittance and reflectance from free standing paint films as well as paint films on substrates were not particularly successful. Current efforts are investigating a simple to

use alternate paint film model that will predict coating transmittances as a function of type and thickness.

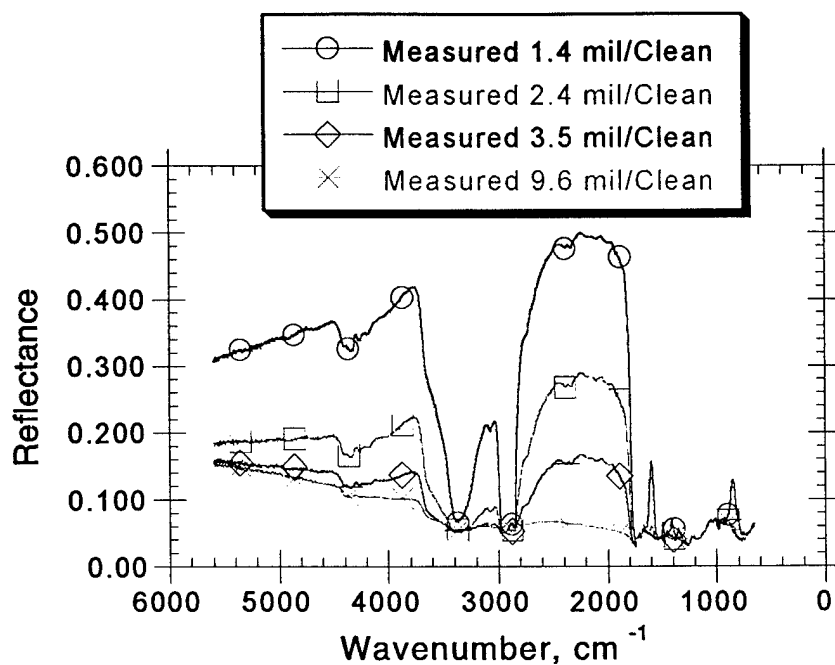


Figure 15 Reflectance of camouflage topcoat on uncorroded aluminum.

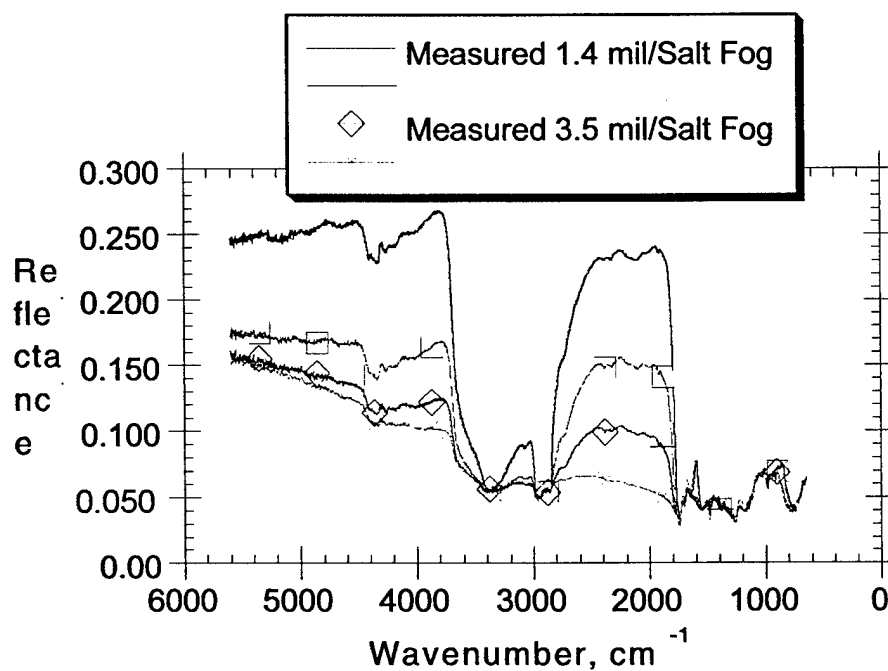


Figure 16 Reflectance of camouflage topcoat on corroded aluminum.

For the prediction of DHR of painted substrates, a simple model based on multiple reflectance's and empirically measured paint transmittances and reflectance's was successfully used. The total reflectance,  $R_t$ , of a paint layer is given by Equation B:

$$\text{Equation B} \quad R_t = R_f + T_f^2 R_s / (1 - R_f R_s)$$

where  $R_f$  is the reflectance of the free standing paint film,  $T_f$  is the reflectance of the free standing paint film, and  $R_s$  is the reflectance of the substrate. This model applies directly to the sensitivity experiments described in this section. However, a question arises as to the validity of the model when applied to a painted substrate where the coating has an intimate contact with the substrate precluding multiple reflections from this boundary. Calculations indicate that for the paint system and substrates considered here, the differences should be relatively small and will not have an adverse impact on the SNDE technique.

Figure 17 and Figure 18 show a measured and simulated DHR for a 1.4 mil thick camouflage coating on a clean aluminum substrate and a corroded substrate, respectively. Considering the approximations made in the measurement of the DHT of this film, the agreement between the measured and modeled curves is remarkably good. Good agreement between the modeled and measured spectra is also made with the other paints as well.

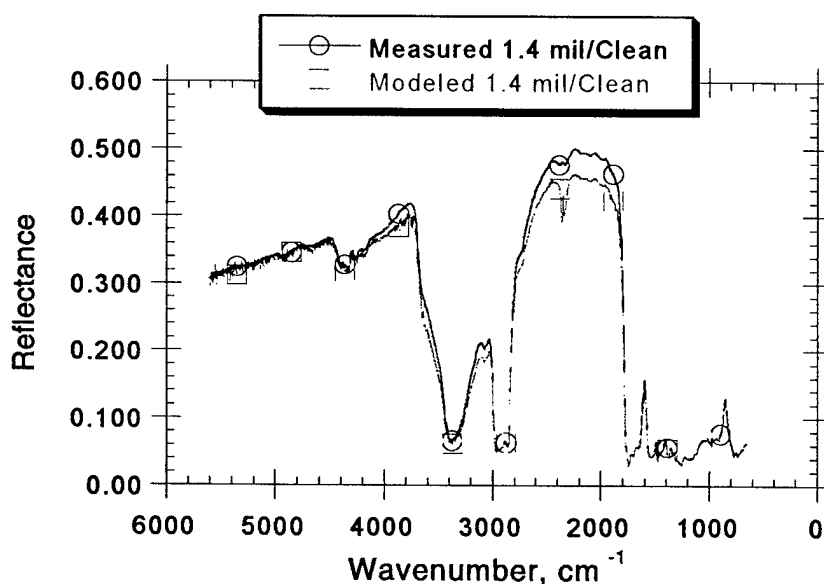
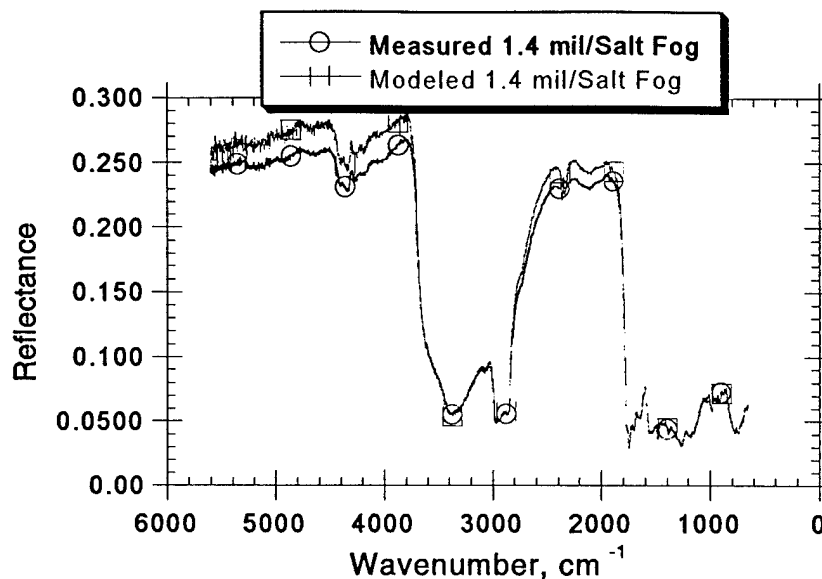


Figure 17 Comparison of measured and modeled reflectance of camouflage paint on uncorroded aluminum.



**Figure 18 Comparison of measured and modeled reflectance of camouflage topcoat on corroded substrate.**

Equation B can be inverted to give the substrate reflectance as a function of the measured DHR of the painted surface. This is shown Figure 19. Except for regions where the paint film is opaque, there is good agreement between the derived substrate reflectance and the actual substrate reflectance measured without a paint coating. The signature of corrosion on the substrate can be clearly seen. However, this analysis can be performed only if there is sufficient transmission of IR light through the coating to provide the needed signal to noise ratio. A better (and simpler) data analysis technique is to ratio the reflectance of a painted uncorroded substrate to the reflectance of a painted corroded substrate. Figure 20 shows this ratio for a series of thickness' of camouflage topcoat. We can see the signature of corrosion even up to a thickness of 10 mil.

For the ratio technique, the reflectance spectra are normalized at the spectral regions where the paint is opaque ( $1100\text{ cm}^{-1}$ ). This eliminates variations due to topcoat weathering and fouling. In addition, signature variation due to different topcoat thickness may be separated from the effects of substrate corrosion. However, a separate thickness measurement may have to be made in order to eliminate this variable. Ultimately, a combination of coatings will have to be probed in order to see to the substrate. This may include some sealant/primers and topcoats.

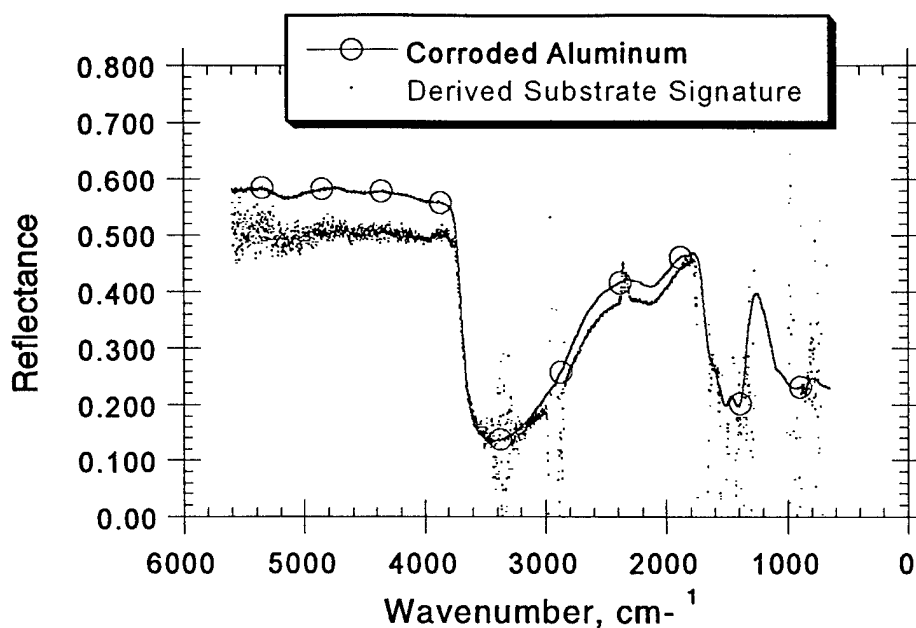


**Figure 19** Comparison of directly measured corroded substrate reflectance and the reflectance derived from DHR measurement of 1.4 mil camouflage painted substrate.

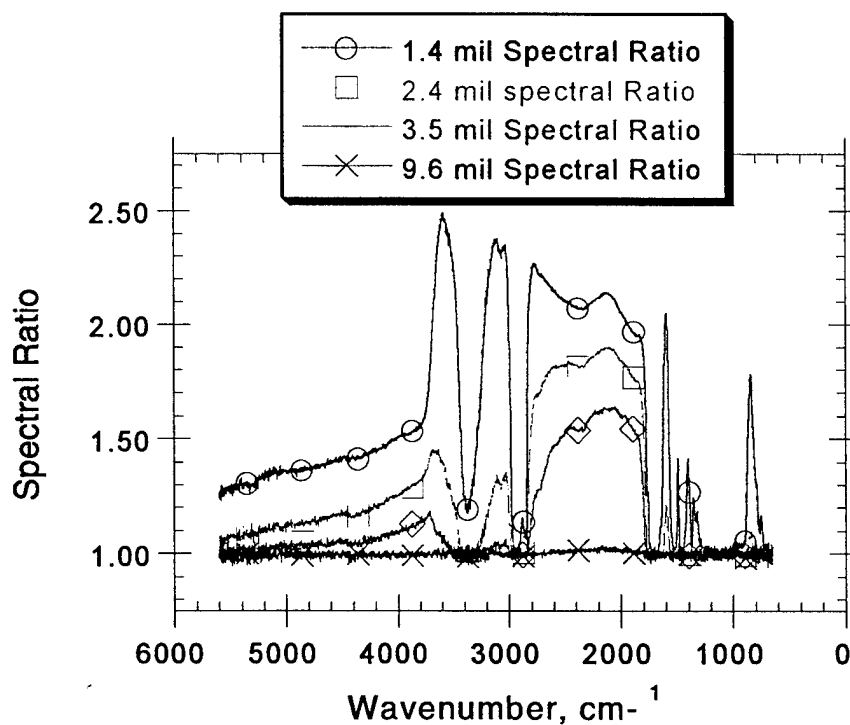


**Figure 20** Spectral ratio of reflectance of painted uncorroded substrate to the reflectance of a painted corroded substrate.

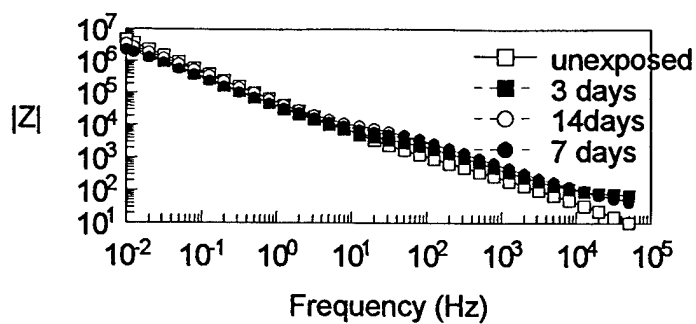
## **ELECTROCHEMICAL IMPEDANCE SPECTROMETRY**

Figure 21 and Figure 22 show the effect of exposure time on the impedance characteristics for the scribed and SAA prepared Al2024 surface. The exposure was for 3, 7 and 14 days in a salt fog atmosphere. As a reference, spectra for unexposed samples are also shown. With the scribed surface, the differences in responses were clearly seen in the Bode plot of the phase angle, *theta*, versus the logarithm of the frequency. A distinct change in the phase angle occurs after the first 3 days at frequencies of 1 to 1000 Hz but little changes thereafter. Changes are also seen in  $Z$ , the impedance magnitude, which increased slightly at frequencies higher than 10 Hz. In contrast, for the unscribed surface in Figure 21, there was little change after 3 days but distinct changes occur after 7 and 14 days as evidenced by the phase angle and the increase in  $Z$ .

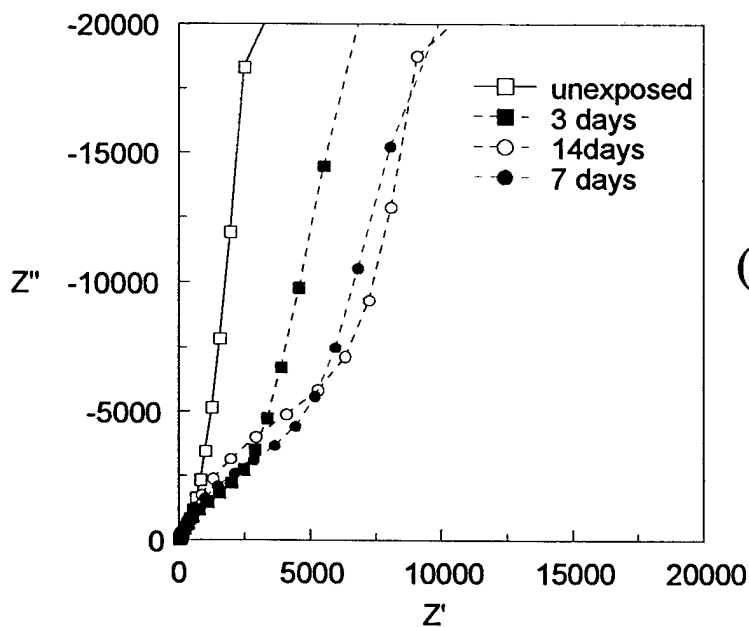
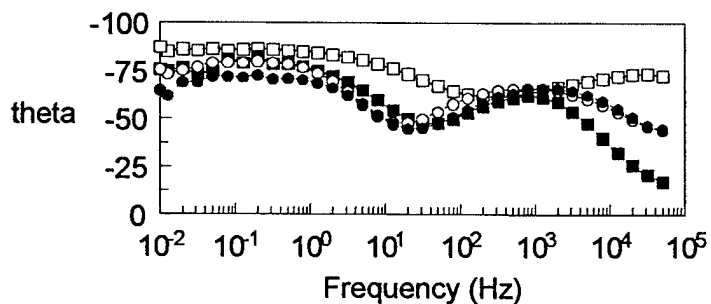
An alternative way of representing the results is the Nyquist plot giving the relation between the real ( $Z'$ ) and imaginary ( $Z''$ ) components of the impedance. The curved portion of the plot after 14 days (Figure 21) at lower impedances is interpreted in terms of the passive film's properties. The linear section at the higher impedances is a function of the electrochemical kinetics and dissolution rate of the sample. The large curved, semicircular section for 14 days shows there is a marked increase in the resistance of the oxide film compared to the results for 7 days, where some resistance increase is apparent. No oxide resistance is apparent for the 3 day exposure.

In the low frequency region (at 0.01Hz),  $Z$  is characteristic of the corrosion resistance of the aluminum oxide barrier film. Mansfield and Kendig [12] have shown that it is not possible to see the changes at these frequencies after short times of immersion. It should be pointed out that during the impedance measurements, areas were exposed to electrolyte for a relatively short period of time, approximately 2-3 hours. In addition, the borate solution is non-aggressive and would tend to help passivate the surface. The results show that the SAA surface on Al2024 reacts in the salt fog and continually changes its electric characteristics. The changes suggest that in the salt fog some sealing of the SAA surface occurs, increasing the oxide resistance while decreasing capacitance. The exposed unprotected metal in the scribe changes rapidly at first also producing a small increase in impedance and suggestive of an improved protective passive film. Figure 23 compares impedances of the scribed and unscribed SAA Al2024 exposed for 14 days.



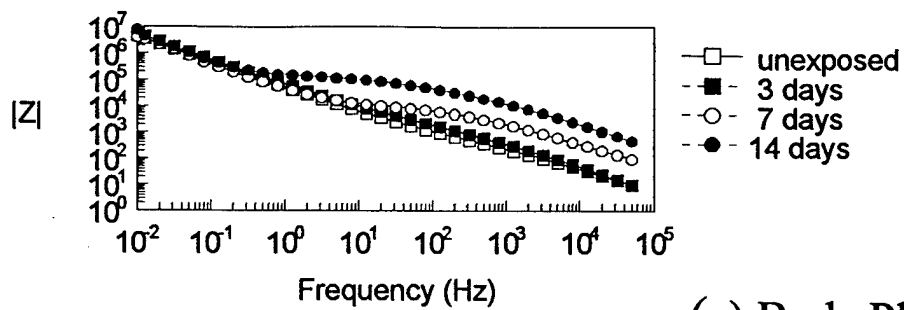


(a) Bode Plot

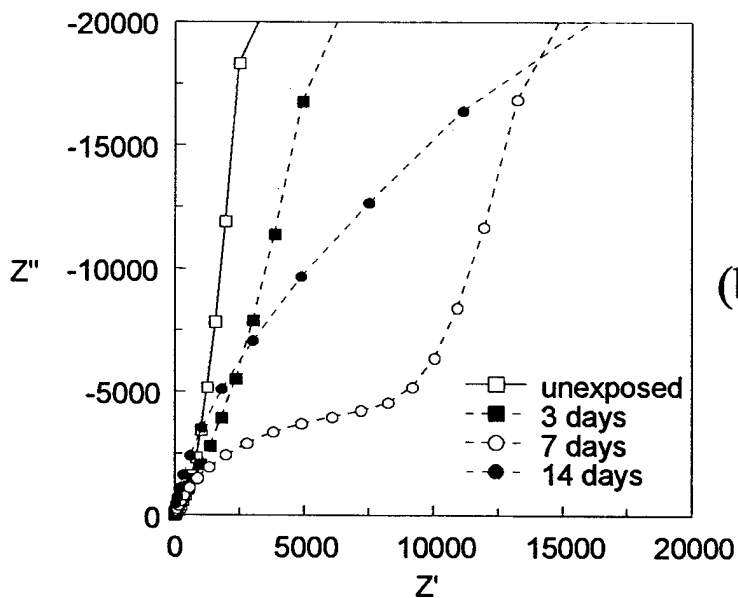
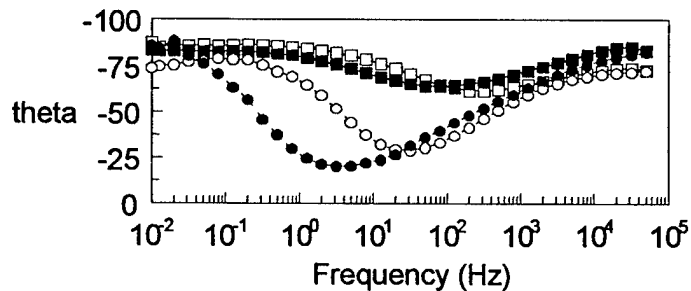


(b) Nyquist Plot

**Figure 21** Impedance spectra on scribed SAA prepared Al2024, exposed to salt fog for 0, 3, 7 and 14 days, measured in borate solution pH 8.4.



(a) Bode Plot



(b) Nyquist Plot

**Figure 22** Impedance spectra on SAA prepared Al2024, exposed to salt fog for 0, 3, 7 and 14 days, measured in borate solution pH 8.4.

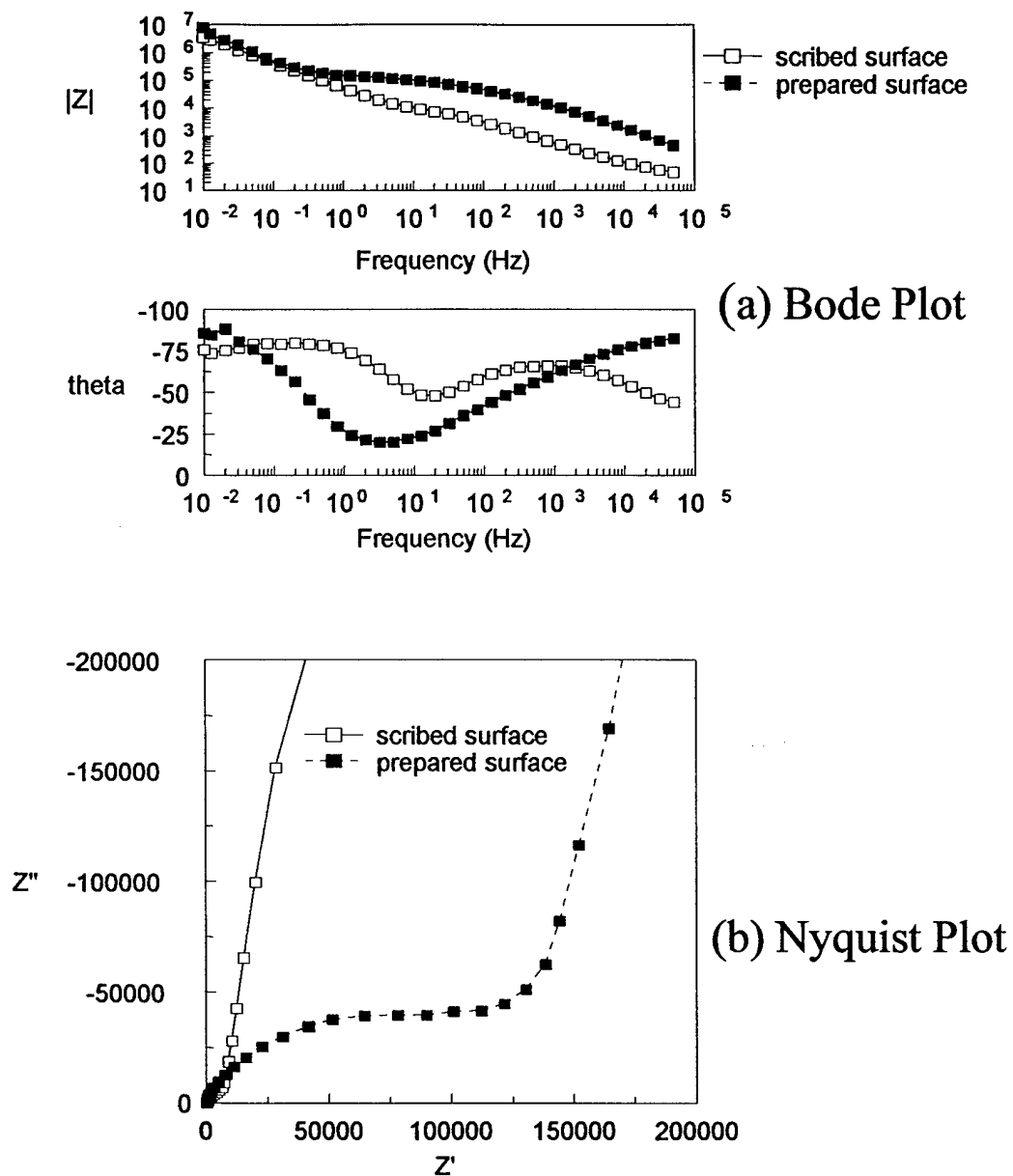


**Figure 23** Impedance spectra for scribed and prepared surface on SAA prepared Al2024, exposed to salt fog for 14 days, measured in borate solution pH 8.4.

The impedance in different electrolytes are shown in Figure 24 and Figure 25 for the Al 2024B SAA surface after 7 days salt fog for scribed and unscribed surfaces respectively. Somewhat similar differences in the response were observed. The highest impedance was for the sulfate and lowest for the borate solutions. This behavior was counterintuitive because the lowest impedance would be expected for the most corrosive, chloride electrolyte.

The differences in the impedances with scribed and unscribed surfaces, shown in Figure 23, were again seen with the SAA on Al2024C. Figure 26 presents impedance data for Al2024C, after exposure for 14 days in salt fog. The impedance measurements were made in 0.1M NaCl. The differences between the scribed and unscribed surfaces are again most obvious in the phase angle plots. The results, as before, indicate a sealing of the SAA during the exposure to salt fog.

A similar conclusion was reached for clad sample in 0.1M  $\text{Na}_2\text{SO}_4$ . Figure 27 shows the impedance at different times of exposure to salt fog. Again, the impedances increased with salt fog exposure, as did the results in Figure 22. There was a difference between that of SAA Al2024 and the clad as continued exposure after 7 days did not lead to any further increases in impedance of the clad. However, the scribed clad (Figure 28) showed a different behavior following salt fog exposure. In contrast to the all the other results after salt fog exposure, its impedance decreased. The reasons for the decrease are not clear and need further investigation. The results, as seen in the Nyquist and impedance magnitude plots in Figure 28, indicate a decrease in the resistance of the passive oxide. This is expected since pure aluminum (representative of the clad) is less susceptible to corrosion in aqueous solutions than Al2024. This is because the potential decreases on exposure, which also allows the passive film to decrease with time. However, the unscribed clad should also have shown similar behavior but did not. Aluminum alloys containing copper show potential increases with time. This leads to increase in passive film thickness. Unfortunately, when the potential increases still further, the pitting potential is reached and pitting corrosion takes place. This condition does not appear to have been reached after 14 days of salt fog exposure. Measurements after longer periods of salt fog exposure are planned to determine when the pitting is apparent on SAA and CCC surfaces.

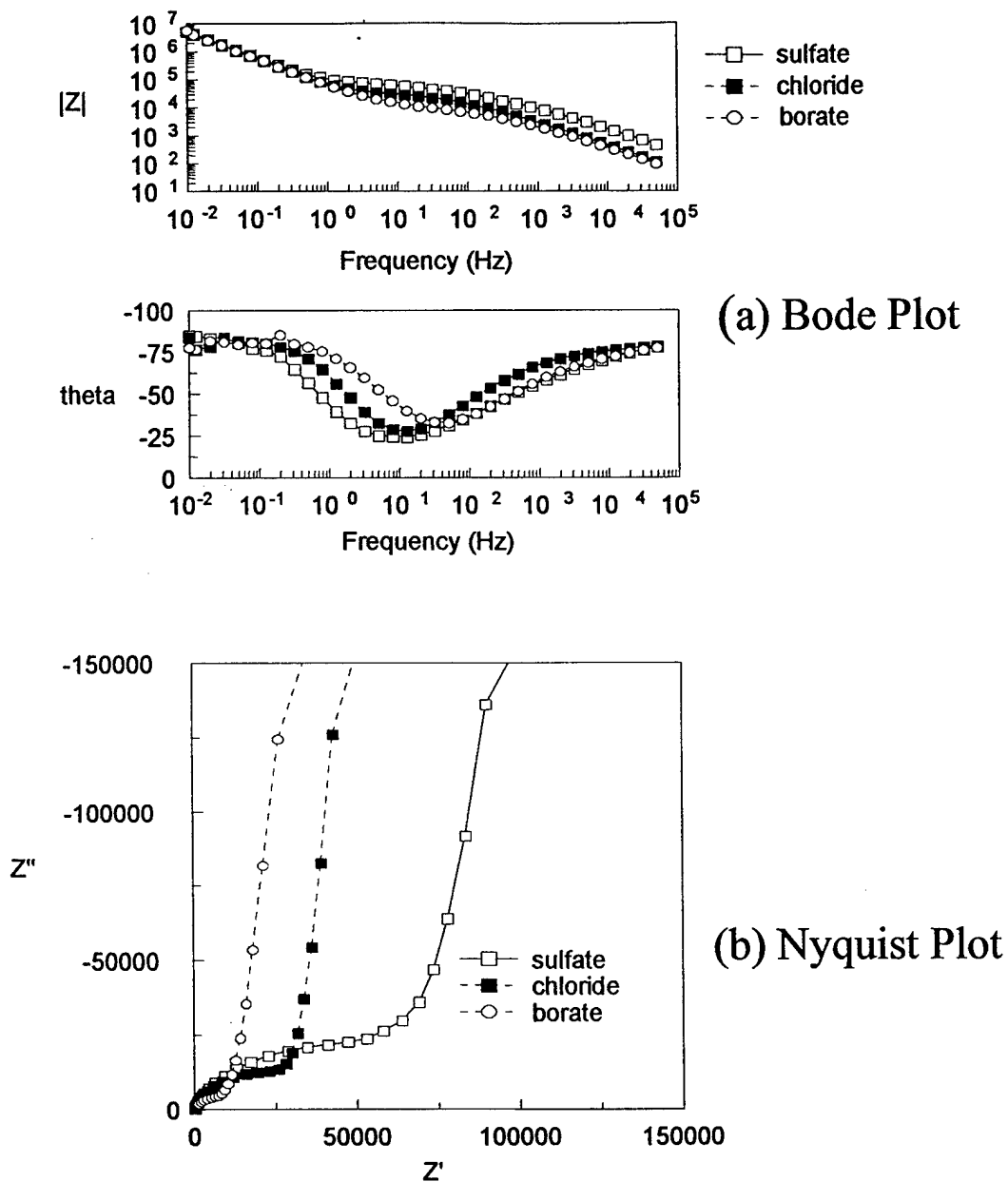
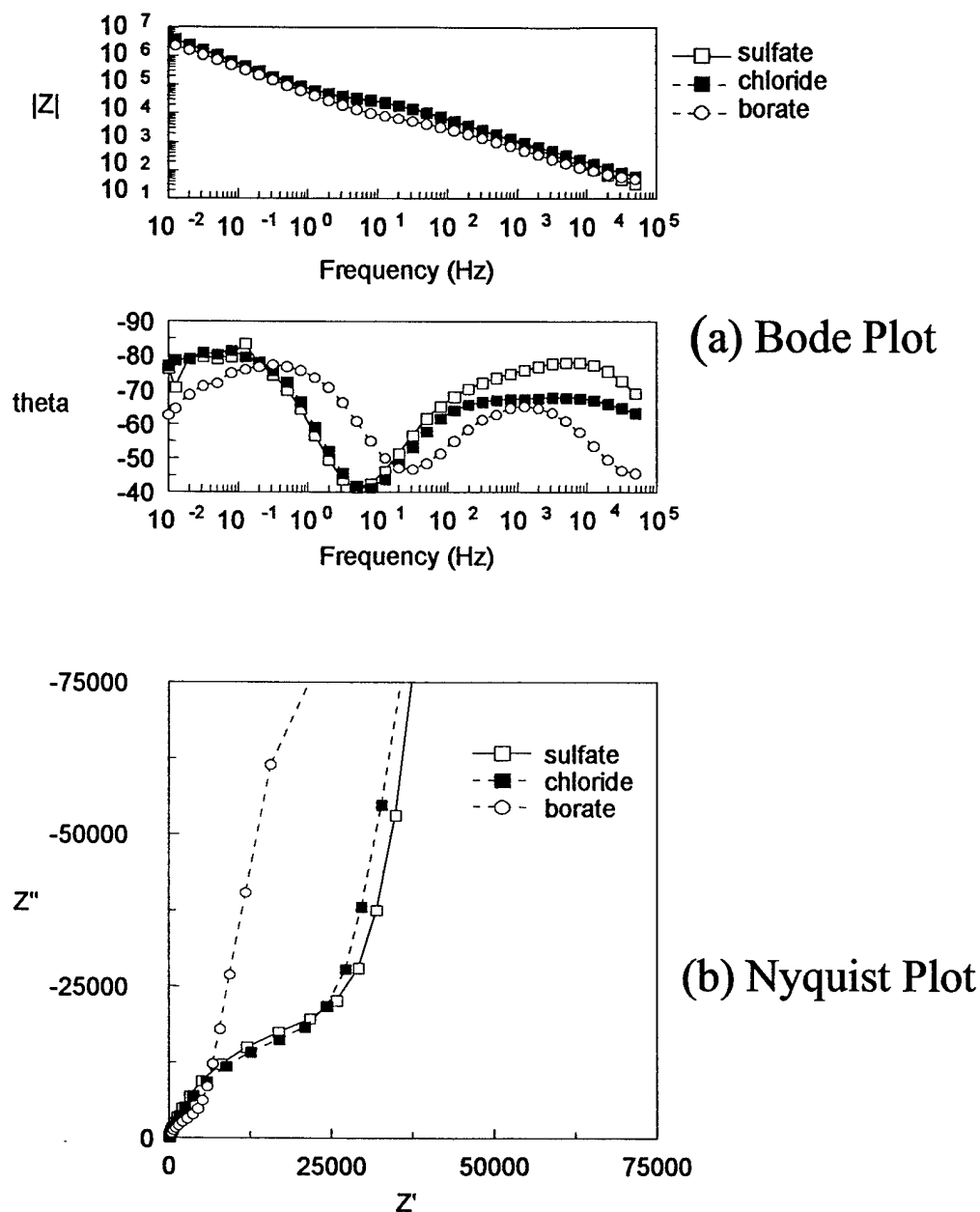
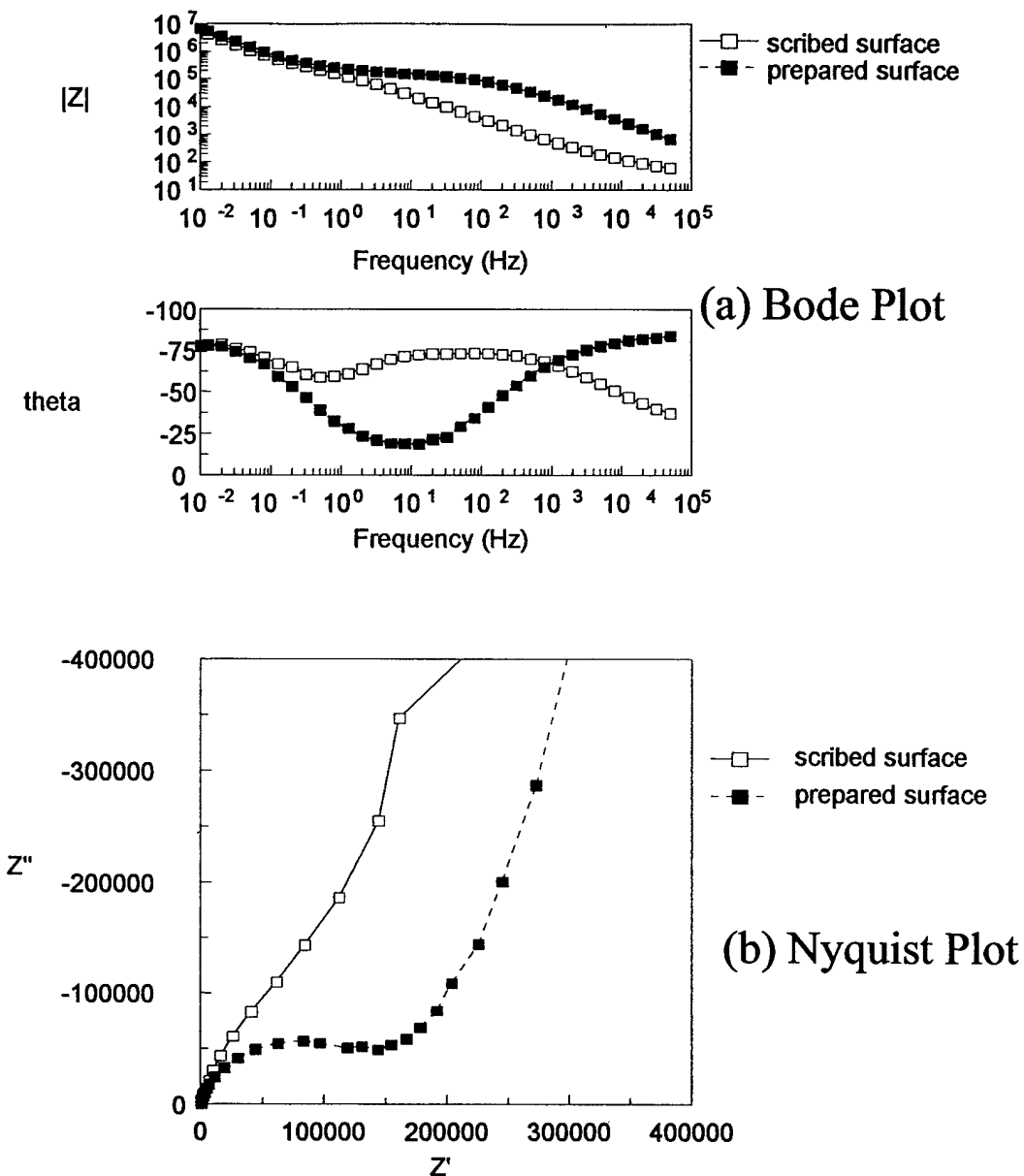


Figure 24 Impedance spectra in borate solution pH 8.4, 0.1M  $\text{Na}_2\text{SO}_4$  and 0.1M  $\text{NaCl}$  on SAA prepared Al2024, exposed to salt fog for 7 days.



**Figure 25** Impedance spectra in borate solution pH 8.4, 0.1M Na<sub>2</sub>SO<sub>4</sub> and 0.1M NaCl on scribed SAA prepared Al<sub>2024</sub>, exposed to salt fog for 7 days.



**Figure 26** Impedance spectra for scribed and prepared surface on scribed SAA prepared Al2024, exposed to salt fog for 14 days, measured in 0.1M NaCl.

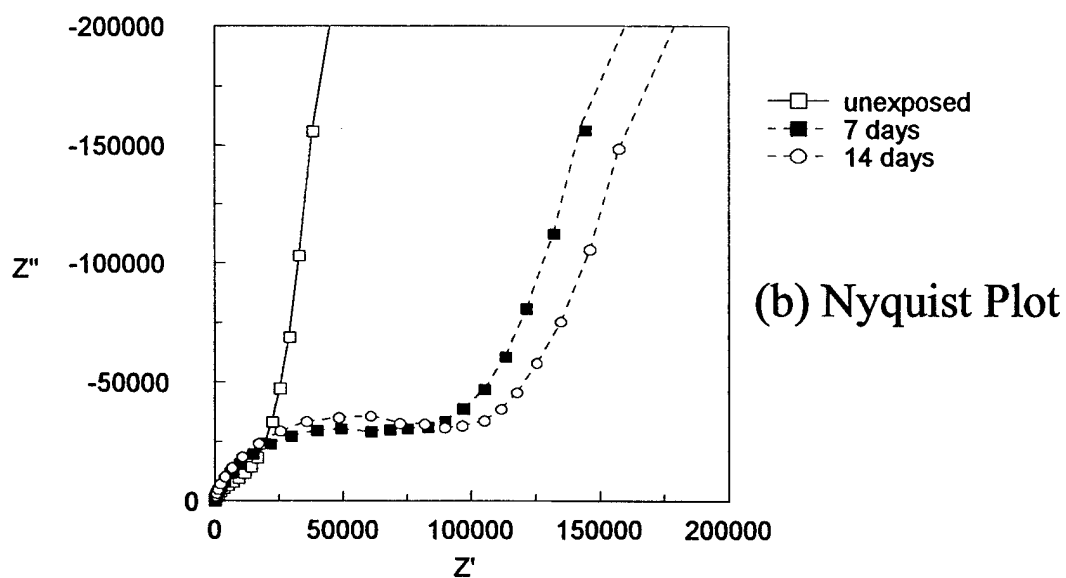
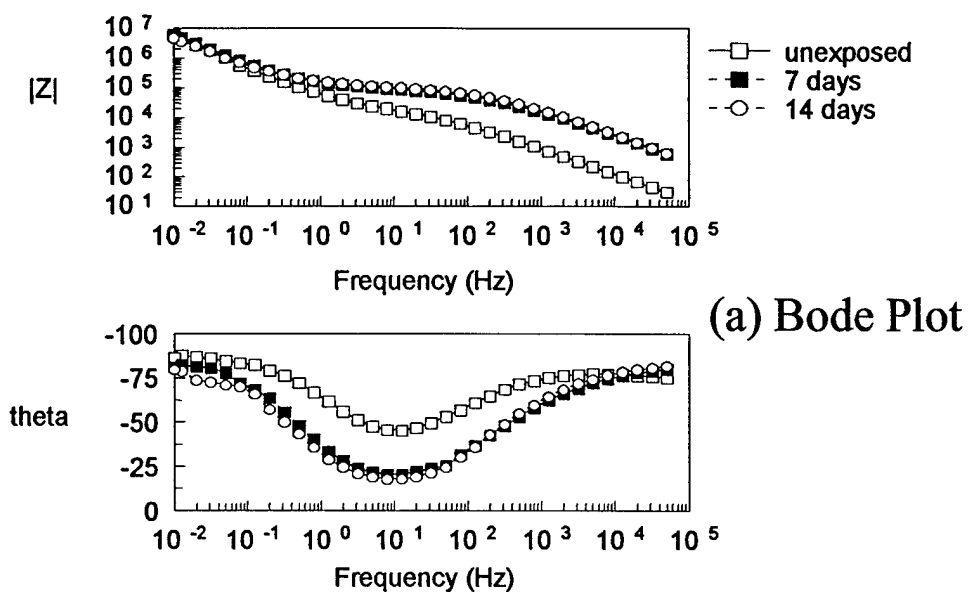


**Figure 27** Impedance spectra on SAA prepared Al<sub>2</sub>O<sub>3</sub>, exposed to salt fog for 0, 7 and 14 days, measured in 0.1M Na<sub>2</sub>SO<sub>4</sub>.



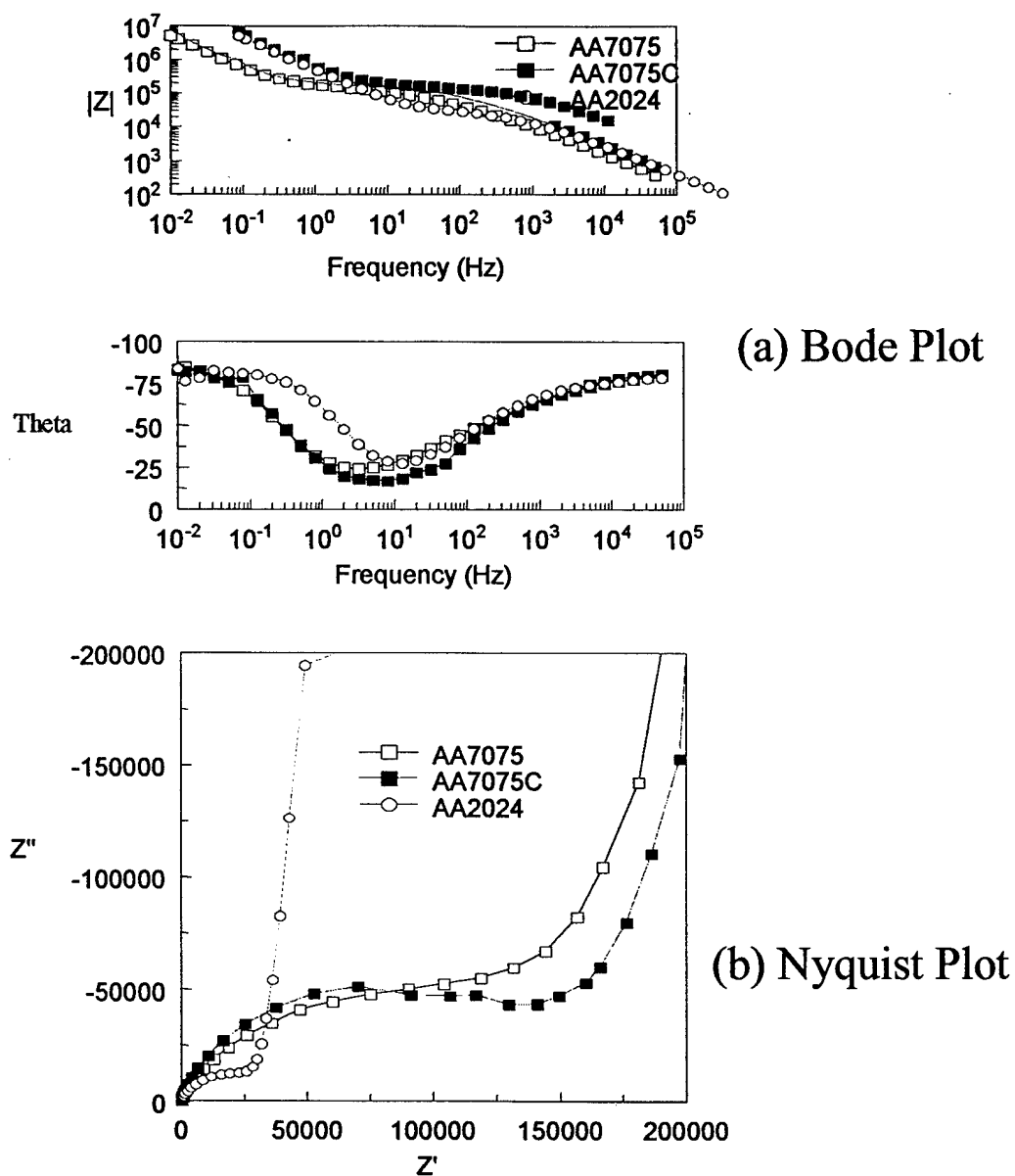


**Figure 28** Impedance spectra on scribed SAA prepared Al2024C, exposed to salt fog for 0, 7 and 14 days, measured in 0.1M  $\text{Na}_2\text{SO}_4$ .

The present study will covers a range of variables and a series of comparisons are required to establish a baseline for their effects on the impedance response. For example, the effect of different alloys and the effect of surface treatments are being established and are reported here. Figure 29 shows a comparison of the impedance response of three alloys, Al7075, the Al7075C, and Al2024. They had had a SAA treatment, and had been exposed 7 days to salt fog. Measurements were made in 0.1M NaCl on the prepared surface of these alloys. They show a small difference in the spectra for Al7075 and its cladding different from that for Al2024. The Al2024 showed the lowest resistance above 0.5 Hz and as seen from both the Bode and Nyquist plots indicating a lower resistance and possibly a lower corrosion resistance of its anodic oxide.

The effect of different surface treatments is shown Figure 30 where a comparison is made between DEOX, SAA and CCC treatments. Bode Plots for unexposed alloys in 0.1M Na<sub>2</sub>SO<sub>4</sub> show higher impedance for Al2024C with SAA surface treatment. The spectra for deoxidized alloy and the alloy with a CCC, are almost identical.

Impedance spectra in 0.1M Na<sub>2</sub>SO<sub>4</sub> for the unexposed, bare and clad Al2024 with different surface treatment are presented in Figure 31. These spectra show that, regarding corrosion resistance, the alloys with surface anodized in sulfuric acid (SAA) have superior behavior compared to the alloys with the CCC. Overall, the sample SAA Al2024C has the highest impedance.

The superior performance is found for SAA Al2024, which were exposed to salt fog for 14 days, compared to the same sample with CCC. Impedance spectra for these samples were obtained in a two-electrode cell and they are shown in Figure 32 in 0.1M Na<sub>2</sub>SO<sub>4</sub>. This data also show that it is possible to obtain a difference in impedance behavior between two different samples in a two-electrode cell.

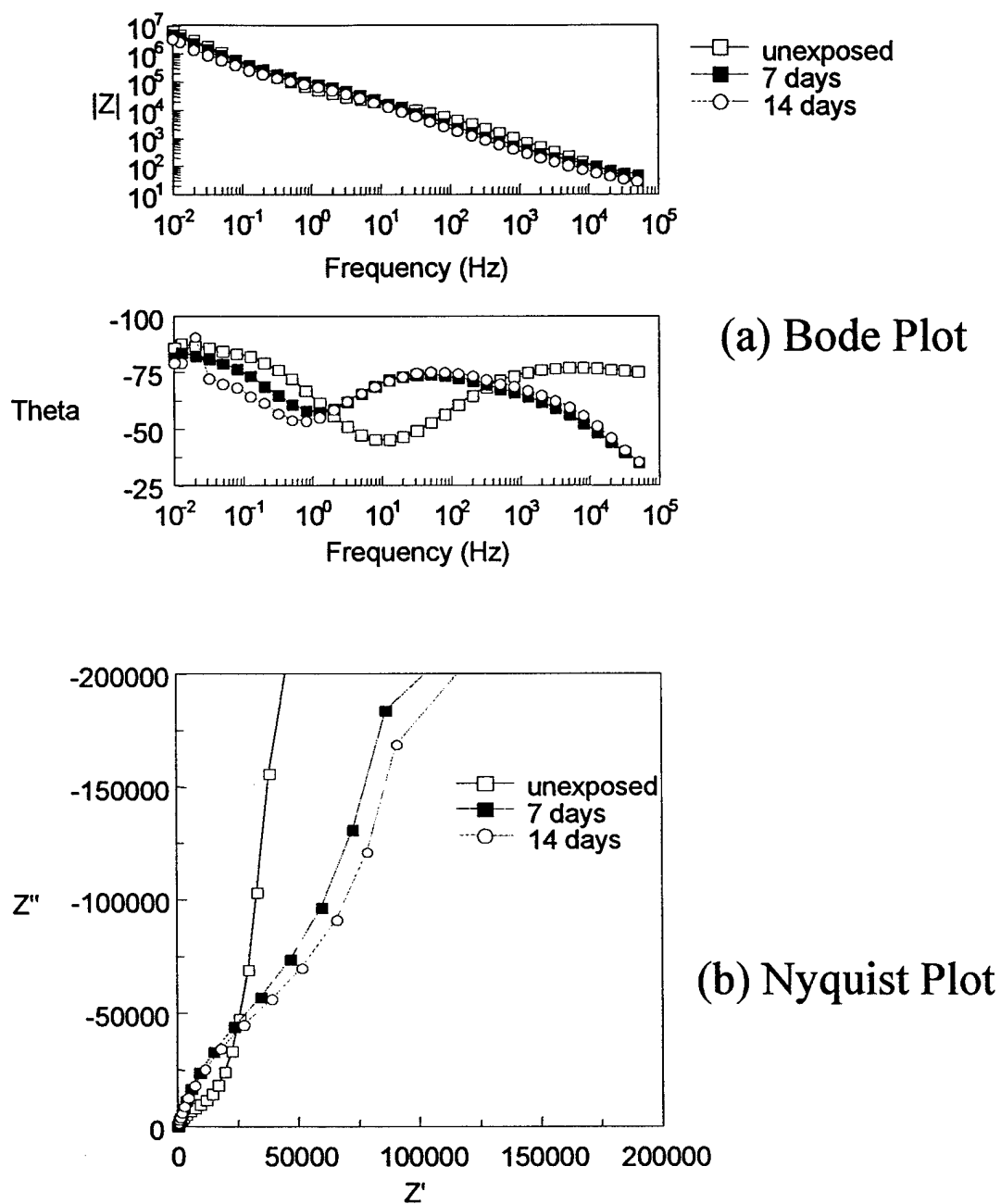
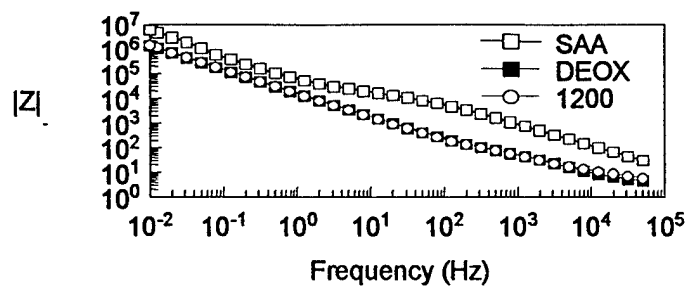
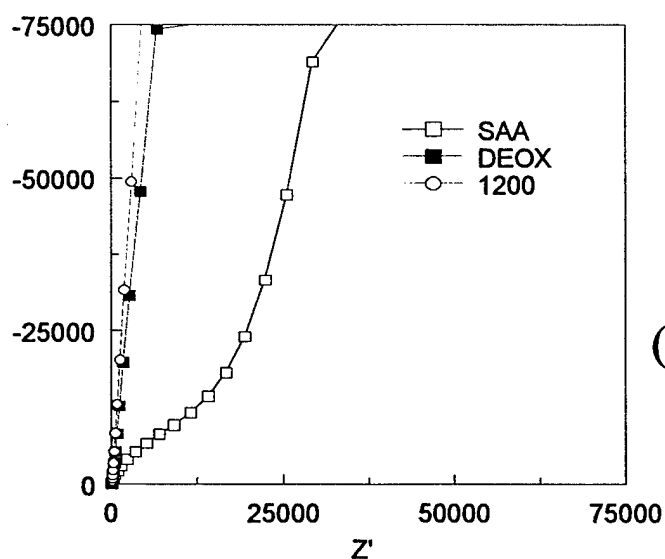
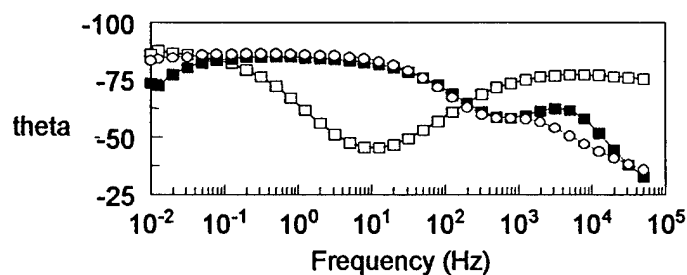


Figure 29 Impedance spectra for SAA prepared Al7075, Al7075C and Al2024, exposed to salt fog for 7 days, measured in 0.1M NaCl.



(a) Bode Plot



(b) Nyquist Plot

**Figure 30** Impedance spectra unexposed Al2024C with surface treatment SAA, DEOX and CCC, measured in 0.1M  $\text{Na}_2\text{SO}_4$ .

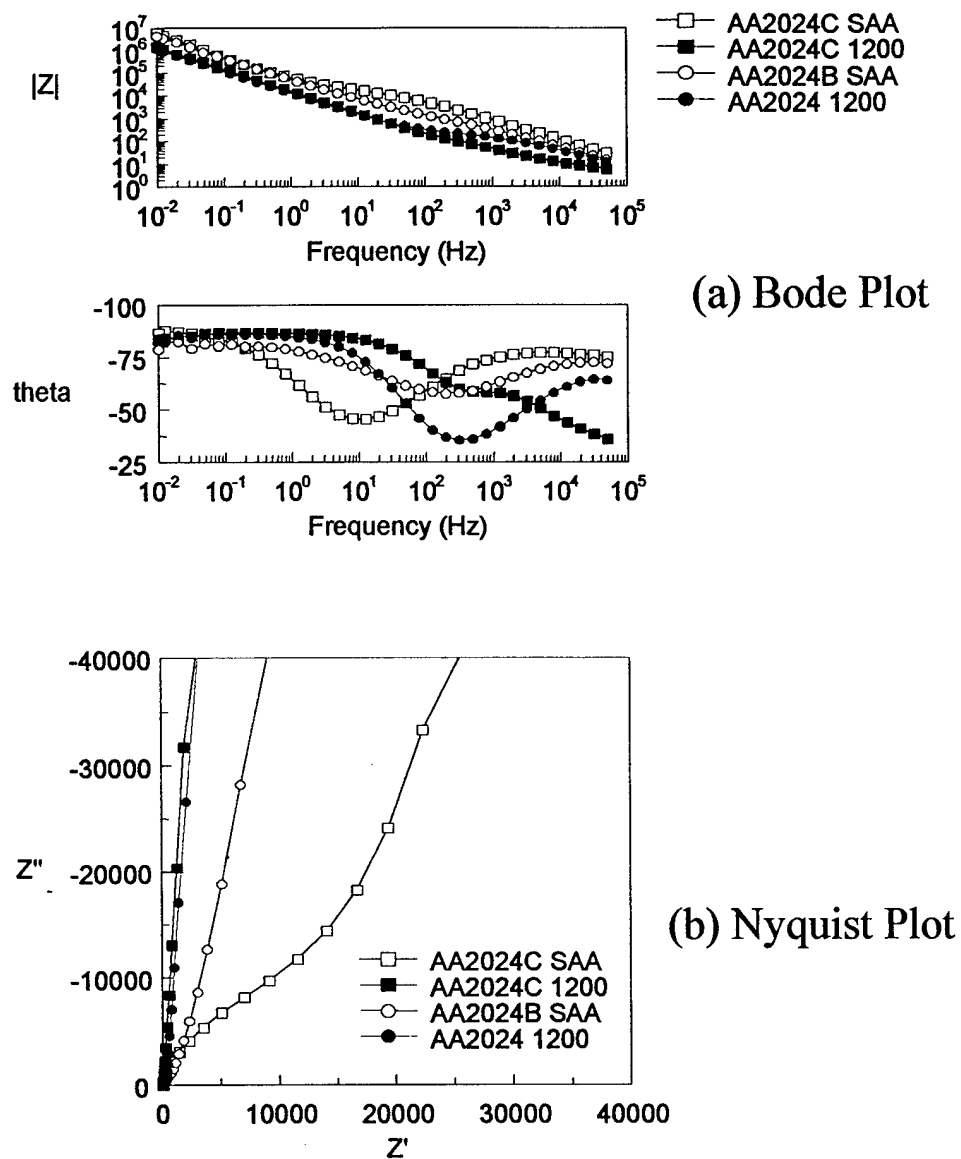
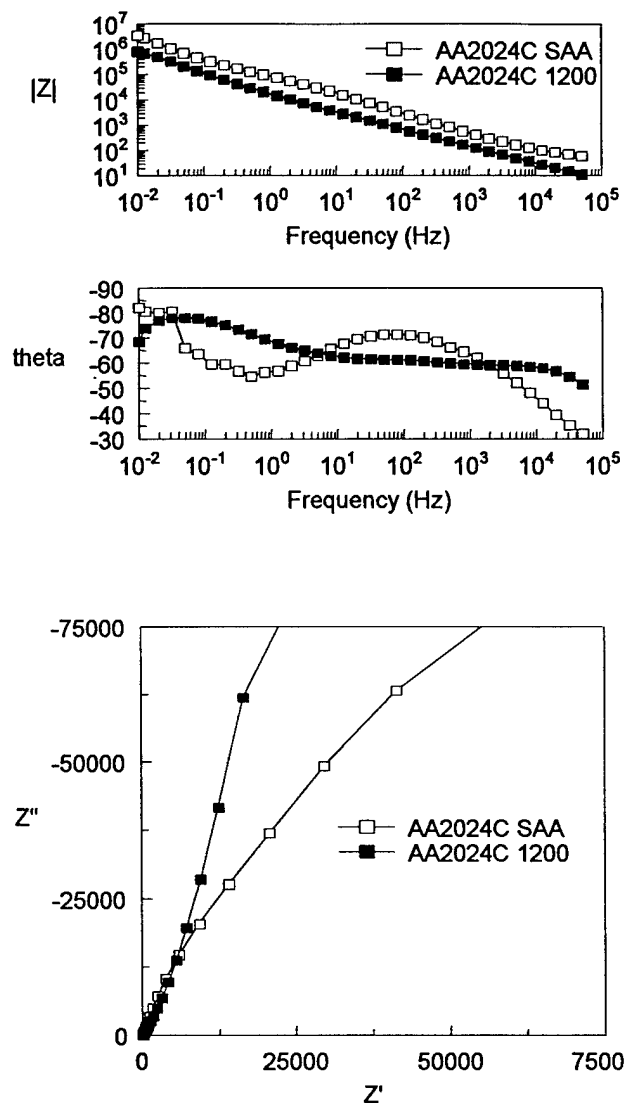


Figure 31 Impedance spectra on unexposed Al2024 and Al2024C, each with surface treatment SAA and CCC, measured in 0.1M Na<sub>2</sub>SO<sub>4</sub>.



(a) Bode Plot

(b) Nyquist Plot

**Figure 32** Impedance spectra on scribed Al2024C prepared with SAA and CCC, exposed to salt fog for 14 days, measured in a two electrode cell in 0.1M  $\text{Na}_2\text{SO}_4$ .

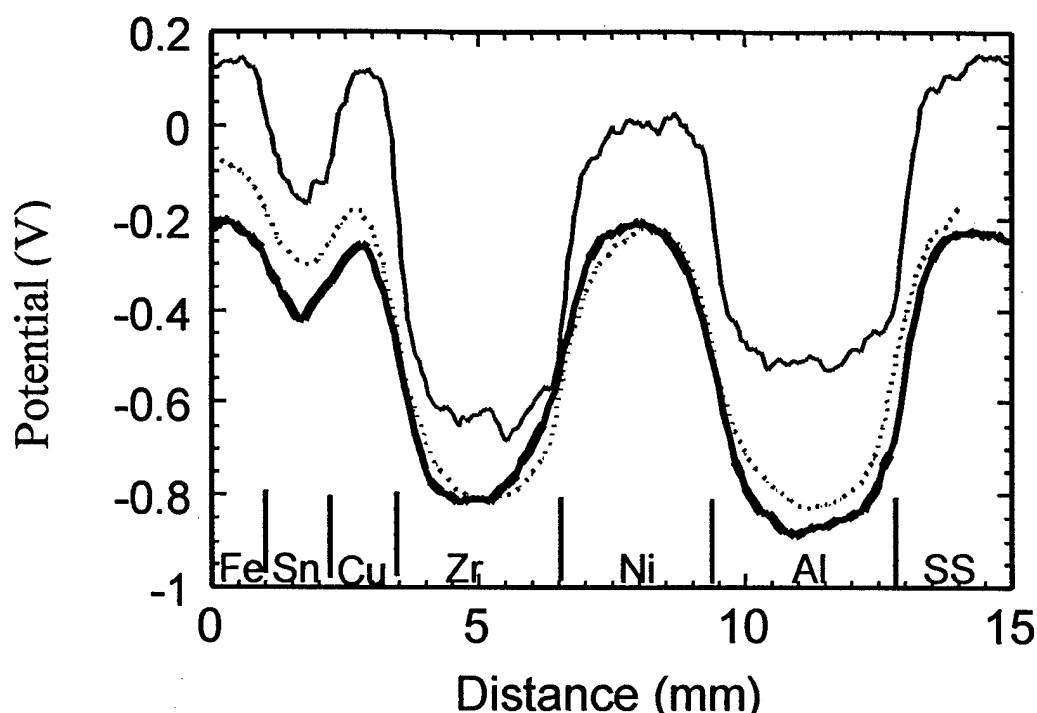


**Figure 33** Scans showing Volta potential variations over a multi-metal sample. (A) Potential measured using Kelvin probe. (B) the beam impinging on the sample; (C) the beam passing over the surface.

### SCANNING VOLTA POTENTIAL MEASUREMENTS

Figure 33 shows a Kelvin probe scan in air over the sample consisting of a series of metal referenced relative to the Ni metal and two measurements made of the Volta potentials for the same sample in the ionized air created by an x-ray beam with a monochromatic x-ray energy of 6.1 keV with a Pt-Ir probe. Measurements in ionized air with the beam impinging on the sample or passing above it and parallel to the surface gave similar results. Comparison of the three curves demonstrates there is a clear relation between the potential variations measured with the Kelvin probe and the direct Volta potential measurements in the ionized air. The potentials over each metal varied in accordance with its electron affinity and with its position in the galvanic series as has been noted previously by other investigators [13,14]. The distinct shifts in potential between the Kelvin probe and ionized gas measurements, is due to a different reference potential. The effect of distance between probe and sample was to reduce the spatial resolution and to decrease the amplitude. However, even at a height of 1 mm where the decrease in amplitude was about

50% changes in potential could still be measured. This contrasts with the Kelvin probe where the probe height must be less than about 0.05 mm from the surface.

Measurements were made on a sample of Al7075 covered with a polyester adhesive tape (3M Type 5) to simulate a painted surface. The metal has been prepared by abrasion down to 600# grade silicon carbide paper. The tape has a 1 mm diameter hole to simulate a defect in a coating. The reference electrode and x-ray beam was scanned across the center of the hole. Figure 34 shows the results for scans, without further treatment, and then after subjecting the sample to corrosion.

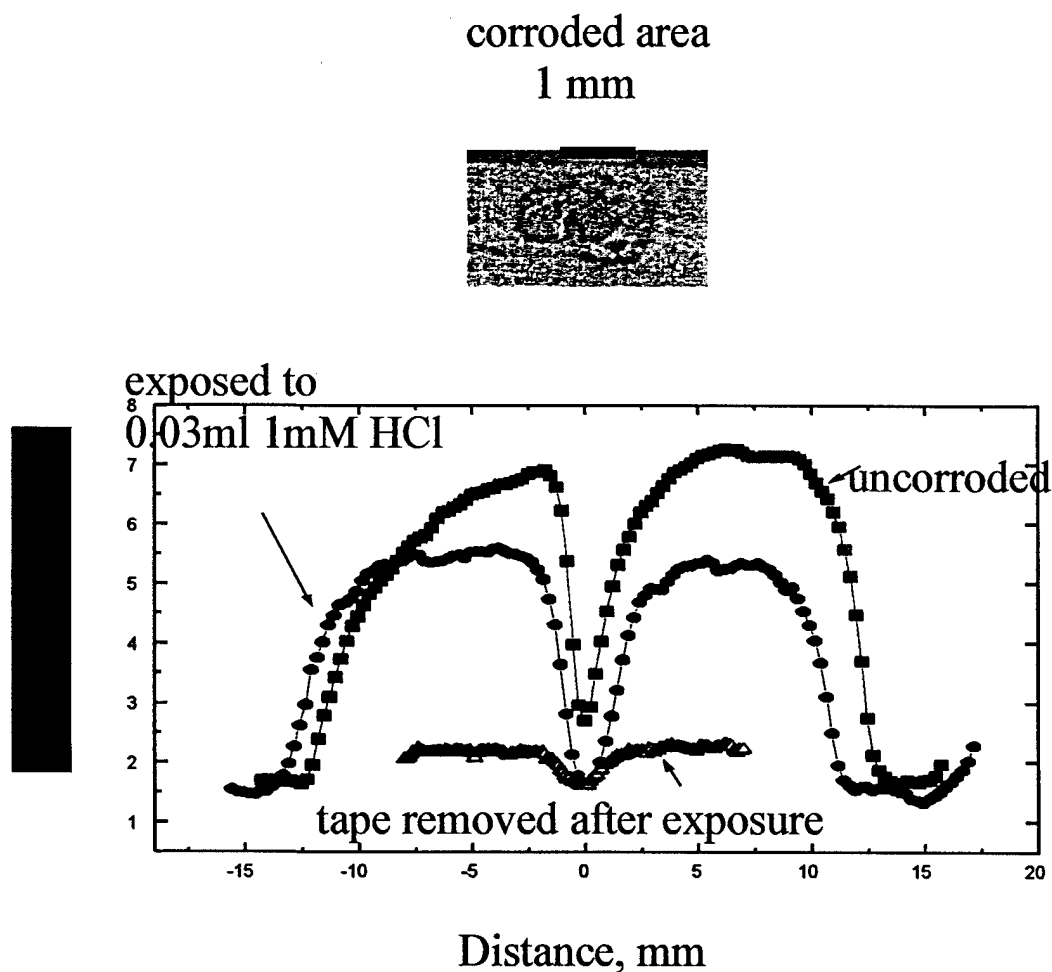


**Figure 34** Volta potential measurements in ionized air for a simulated coating defect.



The measured potentials for the as prepared sample showed potential variations of more than 5 V. These large voltages cannot be attributed to any chemical effects that may produce voltages up to 1.5V. The high voltages were caused by the build-up of charge on the tape. Large decreases in potential were seen when the scan was over the defect in the coating demonstrating that the technique would be extremely sensitive as a method for detecting coating defects. Further work will be carried out to determine if the properties of the polyester played a part in the charging and what effects will be seen with painted surfaces. Humidity may also be important and the charging could be reduced by increased humidity.

The taped sample was then corroded by placing a drop of 0.03 M HCl over the defect in the coating. The apparent size of the defect, as indicated by the width of the potential decrease during the scan, increased and the magnitude of the potential showed a small decrease. The effect of the acid on the coating and the subsequent deposition of corrosion products from the defect was to increase the surface conductivity of the tape. This allowed charge to dissipate into the defect and produced the observed changes after corrosion. Finally the tape was removed from the sample and the surface was again scanned over the corroded area. The corroded region was detected by the Volta potential measurements demonstrating that the technique was sensitive to the presence of corroded areas Al7075.

## CONCLUSIONS AND FUTURE WORK

### **SNDE**

We have made substantial progress in the implementation of the SNDE concept. Specifically, we have developed a database of spectral reflectances of a variety of coatings and coated substrates. In addition, we have modeled the reflectance of corroded aluminum. A data analysis technique was developed to permit the detection of moderate amounts of corrosion at thickness up to 10 mil of topcoat.

While work continues on the completion of the DHR database and SNDE data analysis techniques, we will begin the development of a simple shop based application of the DHR SNDE technique. This will include investigation of the use of fiber optic cable to connect a reflectance head to a spectrometer. Using a limited number of spectral bands as determined by the database, a simple system using an IR source and few selected filters may all that is need to complete this system.

Work will also begin on the wide Area spectral Imaging (WASI) system. This will begin with a thermal IR imaging coupled to a number of IR band pass filters. Images in various spectral regions (transmissive and opaque) will be ratioed to reveal contrast formed by corrosion products and the metal/paint interface.

### **Impedance Measurements**

Probes for the measurement of impedance on coated surfaces have been developed. The results obtained have shown that the impedance methods can clearly detect changes on a range of alloys with different surface preparations with and without scribing to accelerate corrosion. This approach with samples, exposed to standard salt fog and to humidity testing, will be extended. More accelerated corrosion methods will be used to establish the appropriate solutions for use with heavily corroded samples to identify the corrosion sites. Measurements will be made with painted samples where the paint has been undermined by the corrosion process and where corrosion is present and the coating is intact or the surface has been re-coated burying the corrosion.

The impedance measurements to detect the sites of corrosion under intact coatings will emphasize high frequency measurements that respond to

capacitance changes due to thickness increases and changes in dielectric constants due to the growth of corrosion products.

### ***Scanning Volta Potentials Measurements***

Volta potential measurements using conventional Kelvin probe methods and conducting gases have been investigated. The conducting gas technique is significantly more easy to use because of less stringent height restrictions and expected simpler instrumentation.

The conducting gas technique has been found to give high potential measurements because of charging of the simulated painted surface. The high voltages make the method highly sensitive to the detection of defects in coating. However, the effect of the degree of charging of painted surfaces and its effect on the detection of corrosion under painted surfaces must still be investigated in the future.

The conducting gas technique, has used x-rays to create the ionize gas. This approach is not applicable for application to aircraft. Alternative methods will be tested. One approach will be to use a spark source in a confined volume and flow the ionized gas from this source to between the coated surface and scanning reference electrode.

## ACKNOWLEDGMENTS

The authors of this report would like to acknowledge the following individuals for their assistance in defining the objectives of this work as well as assisting in test specimen preparation, experimentation and report writing:

Gordana Adzic, Research Associate, Brookhaven National Laboratory  
Steve Chu, Research Technician, Northrop Grumman, Bethpage, NY  
Rick Doria, Manager, Environmental, Health, Safety and Medical, St. Augustine, FL  
Doug Hansen, Research Scientist, Perkin-Elmer Scientific Instruments, Oak Ridge, TN  
Peter King, Manager, Manufacturing Technology, Northrop Grumman, St. Augustine, FL  
Sonny Lee, Quality Assurance Supervisor, Northrop Grumman, St. Augustine, FL  
John Kimmet, Research Technician, Northrop Grumman, Hawthorne, CA  
John Weir, Lead Material & Process Engineer, Northrop Grumman, Bethpage, NY  
Dave Welch, Quality Inspector-Aircraft Coatings, Northrop Grumman, St. Augustine, FL  
Michael Steele, Sr. Technical Specialist, Northrop Grumman, El Segundo, CA

## REFERENCES

1. D.O. Thompson, and D.A. Chimenti, Review of Progress in Quantitative Nondestructive Evaluation, Vol 16A-16B, Plenum, New York (1997)
2. Dean, S.W. Jr. (1985) Electrochemical methods of corrosion testing. In: *Electrochemical Techniques*, R. Baboian, ed. NACE Publications, Houston, TX. Pp. 193-207.
3. M. Stratman and H. Streckel, *Corrosion Sci.*, **30**, 681 (1990).
4. A. Leng, H. Streckel and M. Stratman, *Corrosion Sci.*, **41**, 547 (1999).
5. S. Yee, R. A. Oriani and M. Stratmann, *J. Electrochem. Soc.*, **138**, 55 (1991).
6. B. Case and R. Parsons, *Trans. Faraday Soc.* **63**, 1224 (1967)
7. T. Smith, *J Applied Physics*, **46**, 1553 (1975).
8. G. C. Smith . J. Fisher and V. Radeka, *IEEE Trans. Nuc. Sci.* **NS-31**, 521 (1984).
9. J. D. Cobine, *Gaseous Conductors*, McGraw-Hill Book Co., Inc., 1941.
10. L. Katz and A. S. Penfold, *Rev. Mod. Phys.*, **24**, 28 (1952)
11. K. W. Jones, W. M.Kwiatek, B.M. Gordon, A. L. Hanson, J. G. Pounds, M. L. Rivers, S. R. Sutton, A. C. Thompson, J. H. Underwood, R. D. Giaque, and Y. Wu, in *Advances in X-ray Analysis*, C.V.Gilfrich, R. Jenkins, J. C. Russ, J. W. Richardson, Jr., P. K. Predecki, Edts., Vol. 31, Plenum Pub. Co., 1988.
12. F.Mansfeld and M. W. Kendig, *J. Electrochem. Soc.*, **135**, 4828 (1988).
13. M. Stratman and H. Streckel, *Corrosion Sci.*, **30**, 681 (1990).
14. P. Schmutz, and G. S. Frankel, *J. Electrochem. Soc.* **145**, 2295 (1998).